JAERI-M
91-209

STUDY ON OPERATIONAL CAPABILITY OF ITER

December 1991

Toshiko NAKAZATO*, Tadanori MIZOGUCHI**
Yasuo SHIMOMURA, Masayoshi SUGIHARA
and Toshihide TSUNEMATSU

日本原子力研究所
Japan Atomic Energy Research Institute

JAERI-Mレポートは，日本原子力研究所が不定期に公刊している研究報告書です。
入手の問合わせは，日本原子力研究所技術情報部情報資料課（〒319-11 茨城県那珂郡東海村）あて，お申しこみください。なお，このほかに財団法人原子力弘済会資料センター（〒319-11 茨城県那珂郡東海村日本原子力研究所内）で複写による実費領布をおこなっております。

JAERI-M reports are issued irregularly.
Inquiries about availability of the reports should be addressed to Information Division Department of Technical Information, Japan Atomic Energy Research Institute, Tokaimura, Naka-gun, Ibaraki-ken 319-11, Japan.

編集兼発行　日本原子力研究所
印　　刷　ニッセイエブロ株式会社

JAERI-M 91-209

Study on Operational Capability of ITER

Toshiko NAKAZATO*, Tadanori MIZOGUCHI**, Yasuo SHIMOMURA
Masayoshi SUGIHARA and Toshihide TSUNEMATSU+

Fusion Experimental Reactor Team
Naka Fusion Research Establishment
Japan Atomic Energy Research Institute
Naka-machi, Naka-gun, Ibaraki-ken

(Received November 21, 1991)

Analyses on design space and operational capabilities are performed for both physics and technology phases of ITER (International Thermonuclear Experimental Reactor). The characteristics of three typical operation modes i.e., full inductive Ignition operation, Hybrid operation using partial inductive and non-inductive current drive and Steady-State operation are systematically studied. It is confirmed that the ignition capability of ITER estimated with the newly derived ITER89-L-mode scaling is, on the whole, reasonable. Ignition capability is also shown reasonable even when it is evaluated with the ITER-H-mode scaling. Effectiveness of the possible extension of the operation (i.e., plasma current and fusion power) for ignition capability is clarified. In the case of hybrid and steady-state operations, beta limit is usually restricting the operation space, especially when the wall loading is high. For both cases, the divertor condition is shown most demanding, which is unacceptably high for high wall loading operation. Two possible methods to extend the steady-state operation space, i.e., impurity seeding and higher magnetic field are examined. The divertor condition could be improved both by the medium-Z ion seeding and the increase of magnetic

---

+ Department of Fusion Plasma Research
* Toshiba Corporation
** Hitachi Ltd.

field. The latter is essential to achieve the operation with higher wall loading e.g., 0.8MW/m^2, for nuclear testing.

Keywords: Operation Scenario, ITER, Ignition Operation, Hybrid Operation, Steady State Operation

JAERI－M 91－209

ＩＴＥＲ（国際熱核融合実験炉）の運転性能の検討

日本原子力研究所那珂研究所核融合実験炉特別チーム
仲里　敏子* ・溝口　忠憲** ・下村　安夫
杉原　正芳・常松　俊秀+

（1991年11月21日受理）

ＩＴＥＲ（国際熱核融合実験炉）の設計パラメータと運転性能についてシステム解析を行なった。検討は三つの代表的運転シナリオ（自己点火誘導駆動運転，ハイブリッド長時間パルス運転，定常運転）について行なった。ＩＴＥＲの自己点火運転の能力は新しく導出されたＩＴＥＲ89－Ｌ－モード則に対しても，従来の各種Ｌ－モード則とほぼ同程度であることが確認された。また新しく導出されたＨ－モード則に対しても同様の評価を行なったところ，十分な自己点火性能を有することが確認された。プラズマ電流と核融合出力を増大する拡大運転により，自己点火の性能はさらに高められることが明らかにされた。ハイブリッド長パルスおよび定常運転に対しては，壁負荷が高い時にはベータ限界が制限条件となり，またダイバータ条件（熱負荷など）が最も厳しい制限条件であることが示された。これらの制限条件を緩和する可能性として中間Ｚの不純物混入とトロイダル磁場増大の二つの方法が調べられ，それぞれ有効であることが示された。

那珂研究所：〒311-01　茨城県那珂郡那珂町大字向山801-1
＋　炉心プラズマ研究部
＊　㈱東芝
＊＊　㈱日立製作所

Contents

目　　次

I. Introduction

The physics design constraints consistent with the various engineering design conditions and constraints, e.g., neutron wall loading, divertor peak heat load, superconducting magnet and so on play an important role in determining the design point of fusion reactor. The design point and operation capability for ITER are investigated by the tokamak system analysis code.

ITER design point has been determined by the evaluation of confinement capability for high Q operation based on then existed L-mode scaling laws (e.g., Goldston, Shimomura-Odajima, Rebut-Lallia, T-10) in the early phase of conceptual design activity. As the design activity is proceeding, new L-mode scaling laws, i.e., ITER89-L mode scaling laws, have been developed by the ITER team [1]. It should be very important to examine the confinement capability with these newly developed L-mode scaling laws. Furthermore, in the last year of conceptual design activity, ITRE-H mode scaling laws have been developed [2], even though they are based only on ELM-free non-stationary H-mode discharges. Examination of the ignition capability with these scaling laws is also of primary importance.

The ITER device can accommodate a number of operation modes.[3-5] This flexibility will be proven advantageous in optimizing the plasma performance for each technical objectives imposed on ITER. Major characteristics are examined for the following three typical operation modes : ignition or high-Q operation with short pulse length of a few hundreds seconds, long pulse hybrid operation with a reasonable Q-value and steady state operation with a marginal Q-value of about 5.

Steady State Operation is very attractive for demo-simulation and for nuclear testing in the Technology Phase. The key requirement for Steady State Operation is revealed to be the compatibility with the demanding divertor conditions due to its high plasma temperature and low density needed to drive the full plasma current by non-inductive current drive.

In this report, ignition capability of the present ITER design point and also the effectiveness of extended operation scenarios in increasing the ignition performance are examined by newly developed ITER-L and H mode scaling laws in section II. Capability of long pulse operation is described in section III. Characteristics of steady state operation and

their possible improvement methods are presented in section IV. Conclusions are summarized in section V.

II. Design Point and Ignition Performance

II-1 Choice of Design Point Based on L-mode Scaling

In the beginning phase of the Conceptual Design Activities (CDA), ITER design point has been determined to achieve the required ignition performance based on the then existing typical L-mode scaling laws such as Goldston(G), Shimomura-Odajima(SO), Rebut-Lallia, T-10 scalings. During the course of the CDA, new L-mode energy confinement scalings have been developed (ITER-power and offset-linear laws). these scaling laws are given as follows;

Power law:

$$\tau_E^{ITER\text{-}P}=0.048I^{0.85}R^{1.2}a^{0.3}\bar{n}_{20}^{0.1}B^{0.2}(A_i\kappa_X/P)^{0.5} \qquad (1)$$

Offset-linear law:

$$\tau_E^{ITER\text{-}L}=0.064I^{0.8}R^{1.6}a^{0.6}\bar{n}_{20}^{0.6}B^{0.35}A_i^{0.2}\kappa_X^{0.5}/P)^{0.5} + 0.041I^{0.5}R^{0.3}a^{0.8}A_i^{0.5}\kappa_X^{0.6} \qquad (2)$$

Here, I(MA), B(T), R(m), a(m), P(MW), $\bar{n}_{20}(10^{20}m^{-3})$, A_i and κ_X are plasma current, toroidal field, major and minor radius, heating power, average density ion mass number and elongation at null point, respectively. Based on these scalings, I-A-B design space analysis (I;plasma current, A;aspect ratio, B;toroidal magnetic field) is carried out to determine the ITER design point. In this analysis, the following assumptions are employed:

Assumptions:

-Maximum field at TF coil conductor	12T,
-Safety factor at 95% flux surface	3.2,
-Distance between the inner plasma edge and TFC conductor at the inner leg	1.15m,
-Helium concentration	10%,

their possible improvement methods are presented in section IV. Conclusions are summarized in section V.

II. Design Point and Ignition Performance

II-1 Choice of Design Point Based on L-mode Scaling

In the beginning phase of the Conceptual Design Activities (CDA), ITER design point has been determined to achieve the required ignition performance based on the then existing typical L-mode scaling laws such as Goldston(G), Shimomura-Odajima(SO), Rebut-Lallia, T-10 scalings. During the course of the CDA, new L-mode energy confinement scalings have been developed (ITER-power and offset-linear laws). these scaling laws are given as follows;

Power law:

$$\tau_E^{ITER\text{-}P}=0.048 I^{0.85} R^{1.2} a^{0.3} \bar{n}_{20}^{0.1} B^{0.2} (A_i \kappa_x / P)^{0.5} \qquad (1)$$

Offset-linear law:

$$\tau_E^{ITER\text{-}L}=0.064 I^{0.8} R^{1.6} a^{0.6} \bar{n}_{20}^{0.6} B^{0.35} A_i^{0.2} \kappa_x^{0.5} / P)^{0.5} + 0.041 I^{0.5} R^{0.3} a^{0.8} A_i^{0.5} \kappa_x^{0.6} \qquad (2)$$

Here, I(MA), B(T), R(m), a(m), P(MW), $\bar{n}_{20}(10^{20} m^{-3})$, A_i and κ_x are plasma current, toroidal field, major and minor radius, heating power, average density ion mass number and elongation at null point, respectively. Based on these scalings, I-A-B design space analysis (I;plasma current, A;aspect ratio, B;toroidal magnetic field) is carried out to determine the ITER design point. In this analysis, the following assumptions are employed:

Assumptions:

-Maximum field at TF coil conductor	12T,
-Safety factor at 95% flux surface	3.2,
-Distance between the inner plasma edge and TFC conductor at the inner leg	1.15m,
-Helium concentration	10%,

-Other impurity species/their fractions physics guidelines [1]

Other important parameter is the neutron wall loading, which affects the selection of design point and will be shown later. Fig. 1 shows the results of the A-I space analysis for the choice of design point with the wall load of 1.0 MW/m^2. Solid lines show the contour of equi-confinement enhancement factor H of the L-mode scaling laws (H=2) on A-I space for various confinement scaling laws. Thick solid line shows the constraint line for the radial build to provide 400 seconds of full inductive burn. Dotted lines show the contour of the constant plasma major radius. It is shown that the design point of the present ITER provides the similar ignition performance for all of the typical scaling laws considered with minimum major radius under the given physics and engineering conditions and constraints.

ITER offset-linear (L-mode) scaling shows the similar tendency to SO scaling on A-I space. On the other hand, ITER power law (L-mode) scaling indicates substantial aspect ratio dependency, but not such a strong dependency as is obtained from Goldston scaling. It is seen that the power dependency between two types of scalings, the power law and offset-linear law, is quite different. The energy confinement time degrades proportionally to the square-root of the net input power, in the power law type scaling case, so that the fusion product, $\langle nT \rangle \tau_E$, is fairly insensitive to the net input power. On the other hand, the power degradation will saturate in the offset-linear type scaling case. Thus, the offset-liner type scalings will offer better confinement capability than the power law scalings for the higher fusion power operation. In this context, the choice of wall load is closely related to these characteristics of the confinement scaling laws in the determination of the design point of ITER, though this choice could be rather arbitrary, especially for the ignition performance. These features are shown in Figs 2 and 3, where the contour of equi-enhancement factor for ITER power and offset-linear scaling laws are depicted for the wall load of 0.8 and 1.3 MW/m^2, respectively. Other conditions are same as those of Fig. 1. The contour of the equi-enhancement factor (H=2) for ITER offset-linear scaling shifts to higher Ip for lower power (lower wall load) and shifts to lower Ip for higher power (higher wall load). However, the contour for ITER power law scaling is almost unchanged with the fusion

power, while, actually, slight improvement in the performance with increasing wall load can be obtained in the power law.

Under the constraint that both two types of scaling laws should provide the same ignition performance for the same fusion power due to the uncertainty of the present confinement scaling laws, and also under the constraint of the minimum major radius, the choice of 1 MW/m^2 of wall load should be a reasonable one for the design point to achieve the specified ignition performance. If we relax some of the above constraints, other choice is, of course, possible. For instance, if we relax the minimum major radius and favor the ITER power law, other design point with higher aspect ratio and lower plasma current (e.g., I=15 MA, A=4) than the present design point can also be possible for the same ignition performance. In this case, by increasing the wall load up to $\approx$ 1.3 MW/m^2, same ignition performance could be recovered, in principle, even if the ITER offset-linear scaling law dominates the confinement. However, due to this larger fusion power required, it is not completely clear that these design points can really provide exactly same ignition performance as the present one, since the larger fusion power may affect the impurity content. Also, the divertor heat load removal should be more difficult in this larger fusion power operation. At any rate, detailed comparisons between these two design points range far and wide, and will be presented elsewhere.

Table I summarizes the typical operation parameters for the standard ignition operation in the present ITER design point.

II-2 Assessment of Ignition Capability with Newly Developed H-mode Scaling Laws

During the last year of the joint work of ITER CDA, ITER H-mode scaling laws have been newly developed. As in the L-mode scaling laws, power and offset-linear type scaling laws are developed, since both types of scalings are found to equally well reproduce the H-mode discharge data. However, expressions for these H-mode scalings are still under development. In fact, only ELM-free H-mode discharge data are included to develop the scaling at present, while, actually, ELMy H-mode discharge will be the most probable candidate for the improved confinement mode in ITER operation. Thus, at present, the emphasis of

this system study will be placed on the performance assessment on the present design point based on the H-mode scaling laws. Then, we will make only a preparatory assessment on the future possible modification and reoptimization of the design point.

Let us first make an ignition performance assessment of the present standard ignition operation parameters. The energy confinement time with H-mode scaling is 5.5 and 5 seconds for power law and offset-linear law, respectively, for the plasma parameters of the standard ignition operation given in Table I, which leads to the required enhancement factors of $H^{IP}/H^{IO}=0.69/0.77$, respectively. These features are shown if Fig. 4, in which the contours of equi-enhancement factor (o.8 for H-mode and 2 for L-mode scaling laws) are depicted on the plane of temperature and plasma current ($T\text{-}I_p$). Thus, we will expect some margin in the confinement capability for the ignition operation when based on the newly developed H-mode scalings. However, it is of primary importance to examine how much margin really remains in the ELMy H-mode scaling, since some confinement degradation has been observed in the experiments.

Next, we will preparatory examine the future possible modification and reoptimization for the design point. The contours of equi-enhancement factor for the H-mode scaling in A-I space are shown in Fig. 5. The solid and dotted lines represent the power and offset-linear H-mode scaling laws, respectively. Although the absolute confinement capability is slightly improved than that evaluated by the L-mode confinement scalings with the enhancement factor of 2, the dependency of H-mode scaling on A-I space is very similar to those of L-mode scalings. Consequently, similar discussions on the choice of aspect ratio can be applied as in the L-mode scalings case.

II-3 Ignition Performance of Extended Operation Scenarios

Considering the uncertainties of physics data base, several extended operation scenarios are prepared to enhance the experimental capability in ITER. Typical scenarios are extended fusion power and plasma current operation. ITER has a capability to produce a fusion power of 1.7GW at the beta limit (Troyon factor G=2.5) with the plasma current of 22 MA. The poloidal field system is prepared to

accommodate this higher beta plasma. As for the extended plasma current operation, ITER has a capability to save a volt second consumption by means of lower hybrid current drive assist during current ramp-up. The poloidal field system is also prepared to accommodate this higher plasma current operation.

Fig. 6 shows the expected extended operation region bounded by the beta limit, fusion power of 2GW and the plasma current of 28MA in the space of fusion power P_f and plasma current I_p. On this region, the contour of equi-enhancement factor lines are depicted to identify the ignition performance of the extended operation scenarios based on ITER L-mode scaling laws.

In the case of ITER offset-linear scaling, the increase of fusion power is equally effective as that of plasma current to enhance the ignition performance, whereas, in the case of ITER power law scaling, the increase of fusion power is less effective than the increase of plasma current. These features are clearly seen in Fig. 6, where the contour of equi-enhancement factors for the power law scaling are much steeper than those of the offset-linear law in P_f-I_p space. For instance, when the fusion power is increased up to 1.7GW, or the current is increased up to 28 MA, the plasma will ignite with the enhancement factor of $\approx$ 1.7 in the case of offset-linear law scaling. In the case of power law scaling, virtually no improvement is obtained by the increase of fusion power, while the required enhancement factor is reduced down to 1.6, if the plasma current is increased up to 28MA.

Note that these extended operation scenarios will only be realized by extending and exploring the operation regime in the course of the machine operation during the physics phase. The possible extent of these extended operations and their effectiveness depend on the exploration of the respective key issues, which include considerable uncertainty in the present data base, for each of the extended operation scenario. In fact, the divertor heat removal is the key issue for the extension of fusion power and the possible amount of the volt-second saving by LH wave should determine the possible extent of the plasma current. According to the present data base [6], about an equal amount of resistive volt second consumptions could be saved by LH assist at the largest without changing the ramp-up time significantly, which enables up to about 28MA of plasma current ramp-up. Another key issue for the extension of the plasma current to be effective should be to prevent

the confinement saturation associated with the lower safety factor than 3. Possible causes of the confinement saturation are speculated as the sawtooth and power deposition profile effects. The latter cause should be removed due to the intrinsically central heating nature of α-heating in ITER, and the former cause could also be removed by the profile control with LHCD prepared in ITER.

These extended operations will be performed in a limited number of shot. In addition, the pulse length will also be restricted due to the higher divertor load, smaller volt-second capability for flat top as well as the finite resistive skin time to maintain the necessary current profile for the suppression of sawtooth. Although there are such restrictions and concerns for these extended operations, design effort should be done to support the realization of these scenarios, since the benefit in extending the experimental capability will be significantly large if these scenarios are actually realized and effective.

III. Capability of Long Pulse Operation

In the technology phase, essential point in the operation scenario is to prolong the burn time with a reasonable neutron wall load to attain the required neutron fluence for the nuclear testing. It is considered that the reasonably minimum wall load is about 1 MW/m2 at least in the testing region (near the torus midplane). The required fluence for the blanket testing is considered as about 1 MWa/m^2, and this requirement is to be achieved by long pulse operation with non-inductive assistance. This operation scheme is not only desirable for the data base of DEMO, but also demanding for the practical reason of the machine operation. In fact, the pure inductive burn pulse length of 400 seconds are too short, since about 80000 pulses are necessary to accomplish the required fluence, which leads to a serious fatigue problem of the machine.

Physics and engineering constraints, which essentially determine the long pulse operation regime are energy confinement, beta limit, divertor condition, wall loading and installed total current drive power. Let us first examine quantitatively how these various constraints determine the operation regime with leaving the constraint of divertor condition for a while. Fig. 7 shows the contour of the equi-burn time on

the confinement saturation associated with the lower safety factor than 3. Possible causes of the confinement saturation are speculated as the sawtooth and power deposition profile effects. The latter cause should be removed due to the intrinsically central heating nature of α-heating in ITER, and the former cause could also be removed by the profile control with LHCD prepared in ITER.

These extended operations will be performed in a limited number of shot. In addition, the pulse length will also be restricted due to the higher divertor load, smaller volt-second capability for flat top as well as the finite resistive skin time to maintain the necessary current profile for the suppression of sawtooth. Although there are such restrictions and concerns for these extended operations, design effort should be done to support the realization of these scenarios, since the benefit in extending the experimental capability will be significantly large if these scenarios are actually realized and effective.

III. Capability of Long Pulse Operation

In the technology phase, essential point in the operation scenario is to prolong the burn time with a reasonable neutron wall load to attain the required neutron fluence for the nuclear testing. It is considered that the reasonably minimum wall load is about 1 MW/m2 at least in the testing region (near the torus midplane). The required fluence for the blanket testing is considered as about 1 MWa/m^2, and this requirement is to be achieved by long pulse operation with non-inductive assistance. This operation scheme is not only desirable for the data base of DEMO, but also demanding for the practical reason of the machine operation. In fact, the pure inductive burn pulse length of 400 seconds are too short, since about 80000 pulses are necessary to accomplish the required fluence, which leads to a serious fatigue problem of the machine.

Physics and engineering constraints, which essentially determine the long pulse operation regime are energy confinement, beta limit, divertor condition, wall loading and installed total current drive power. Let us first examine quantitatively how these various constraints determine the operation regime with leaving the constraint of divertor condition for a while. Fig. 7 shows the contour of the equi-burn time on

the space of plasma current Ip and temperature T with rather small addition of the external current drive power for the same fusion power as the ignition operation. Since the additional heating power is applied, some confinement margin is obtained at the original ignition operation point (Ip=22 MA, T=10 keV), while virtually no increase of the burn time is available due to such small addition of CD power. However, the contour of equi-enhancement factor shift to the lower Ip region due to the additional power. Consequently, when the operation point with lower Ip and lower temperature on the contour of equi-enhancement factor is chosen, the burn time can be somewhat increased due to the lower loop voltage at higher temperature as well as the reduced volt-second for current ramp-up. Note that the additional power is much more effective for offset-linear scaling than the power law scaling, so the most restricting constraint in this case is the latter one. Beta limit is not restricting, i.e., G=2.5 is below the H-P=2 constraint contour. Maximum available burn time is about 1000 seconds at T=14 keV and Ip=20 MA.

To prolong the burn time further, the constraint of confinement must further be relaxed by increasing the additional current drive power, which inevitably decreases the Q value. At the same time, the constraint of beta limit must also be relaxed from G=2.5 to G=3.0, since the contour of G=2.5 is quite close to that of confinement constraint as is shown in Fig. 7. With these relaxations of the constraints, we obtain more than 4000 seconds of burn time as is shown in Fig. 8, where maximum available current drive power of 115 MW is injected and the fusion power is slightly increased to attain the Q value of 10. In this case, the constraining condition is the beta limit (G=3) for higher temperature and the confinement for lower temperature, respectively, and the burn time of more than 4000 seconds can be attained in the higher temperature region with the constraint of beta. Although the dominant effect for the increase of the burn time comes from the reduced plasma current due to the relaxation of the confinement, some effect also comes from the decreased loop voltage due to the increased current drive power. Note that no steady state operation region does appear with the relatively high Q value and high neutron wall loading due mainly to the high plasma density for high fusion power, which reduces the driven current with the available maximum drive power.. In this case, several adequate operation points are considered from the

view point of each constraining condition. An adequate operation point is b1 for the best divertor condition, b2 for the longest pulse duration and b3 for the best confinement margin.

To prolong the burn time even further, the constraint of beta must be relaxed by decreasing the fusion power, which simultaneously increases the driven current somewhat due to the reduced plasma density. This result is shown in Fig. 9, where fusion power is decreased down to 0.75 MW with the resultant reduction of Q value down to 6.5. Even a steady state operation region appear fairly close to the contour of confinement constraint. The operation point c1 is more severe than c2 with respect to the divertor condition due to its higher temperature and lower density, while the confinement margin for c1 is larger than c2.

Let us now examine the divertor conditions for several of the typical operation points in Figs 8 by using the simplified Harrison-Kukushkin model for divertor heat load analysis [7]. The HK model predicts that the divertor peak heat load is proportional to $P_{div}^{14/9}/n_e^{7/9}$, where P_{div} is the total net input power flowing into the divertor region and n_e is the average electron density of the main plasma. The coefficient is adjusted to the results of the standard ignition operation. Divertor peak heat load for the standard ignition operation is estimated to $9.1 MW/m^2$ at the outer divertor plate including a physics peaking factor. Note that these results show only relative tendency because of the incompleteness of the simple analytic model and the lack of experimental validation of the model. Main parameters characterizing the divertor condition and the resultant divertor conditions obtained by the simple analytic model for the case of Fig. 8 along the contour of beta constraint are shown in Fig. 10. Both divertor peak heat load and divertor temperature increase as the operation temperature increases due to the decrease of the electron density, though they become saturated as increasing the temperature for this constant fusion power operation, which attributes from the saturation of the decrease of density due to the reduction of the increment of fusion reaction cross section with the increase of temperature.

Table II shows the major parameters of the typical hybrid operation scenarios as well as the reference ignition operation scenario for comparison.

IV. Steady State Operation

IV.-1 Operation Space and Impact of Wall Loading for Steady State Operation

In this section, we will examine the characteristics of the operation space for steady state operation and the impact of the choice of neutron wall loading on the characteristics of the space. Let us choose the limiting constraints for the operation space as follows;

$H_{ITER\text{-}P}$	<2.0
$H_{ITER\text{-}OL}$	<2.0
Troyon G	<3.0
q	>3
Q	>5

The last constraint is not necessarily obvious one, while this should be regarded as the constraint for the required external current drive power, which can be specified by Q value and the wall loading. Other important constraints for the steady state operation, such as divertor heat load, bootstrap current fraction and so on, are to be examined on the obtained operation space. We will call this operation space as Operation Space I (OpeS.I).

As will be shown later, the Operation Space I is not such broad, and it is rather difficult to identify the attractive steady state operation point. Thus, we will examine the case with more optimistic constraints for some of the above constraints as follows. First, we will extend the upper limit of $H_{ITER\text{-}P}$ up to 2.2, which could be supported by the H-mode experiments in JET and ASDEX, though steady-state H-mode scaling with ELMs is still under development. Second, we will extend the upper limit of G value, which is based on some possible uncertainty in a beam pressure contribution to MHD beta limits. It is not clear at present whether only a perpendicular component of the injected beam pressure may account for the MHD beta limit or the entire beam pressure may contribute to them. As rather optimistic constraint, we will assume that only one third of the beam pressure to contribute to the toroidal beta limit. Thus, we will employ rather optimistic constraints for energy confinement and beta limit to examine the extended operation space, called Operation Space II (OpeS.II). These

constraints are summarized as follows;

H_{ITER-P}	<2.2
$H_{ITER-OL}$	<2.0
Troyon G*	<3.0*
q_φ	>3
Q	>5

Here, G* includes only one-third of the beam pressure.

From nuclear testing requirement, higher neutron wall loading is more desirable for the technology phase operation. It is considered that the minimum wall loading requirement is $\approx 1 MW/m^2$ at the testing region. The peaking factor of neutron wall loading is about 1.6, and, thus, the minimum average wall loading is about 0.6 MW/m^2. Since the choice of wall loading has a great impact on the steady state operation space, we will first examine the impact for various values of wall loading.

Fig. 11 shows the steady state operation space on T-Ip plane, for the average wall loading of $0.8MW/m^2$. Fig. 12 shows the contours of the current drive power in the case of $0.8MW/m^2$. Operation space is bounded by the constraint of beta limit and the minimum Q value of 5. Here the contours of constant Q-value on Ip and T plane are exactly same as those of auxiliary heating power, since the fusion power is constant in this T-I_p plane. The operation space is, for the present, bounded by the contour of Q=5, but, actually, the required current drive power can easily become excessively large for the operation with higher neutron wall loading as will be shown later. The operation with reduced plasma current leads to the associated reduction of the required current drive power. Increase of the bootstrap current fraction serves somewhat to the reduction of the required drive power. As increasing the operation temperature, the current drive efficiency becomes higher, which again reduces the required current drive power. As a result, the required current drive power has the dependency on Ip and T as shown in Fig. 12. For the operation within the OpeS.I, plasma current must be larger than 17MA and operation temperature be higher than 15keV. Current drive power required is from 160MW to 180MW. Achievable Q value is only 5 to 6 as shown in Fig. 13. The fraction of bootstrap current is less than 30%. Since the total heating power, summation of alpha power, current drive power and Joule power, is quite large, the divertor peak heat load will exceed $35MW/m^2$ as shown in Fig. 14. The steady

state operation with the wall loading of 0.8MW/m^2 is very difficult since the current drive power required is too large (note that the installed power is 75 MW for NB and 45 MW for LH), and the divertor heat load is also too large.

If one could operate on the OpeS II, where only one-third of the beam pressure is taken into account for the beta limit, the operation current can be reduced. As a result, the required current drive power is reduced to 120MW and Q value is improved to about 8. Therefore, the improvement of beta limit gives substantial impact on the steady state performance with rather higher wall loading. Although the divertor peak heat load is also improved by this extension of beta limit, the degree of improvement is rather small and the value is still nearly 30MW/m^2.

Fig. 15 shows the operation space for the case of 0.6MW/m^2 wall loading. In this case, the required minimum current at a given temperature is bounded by the confinement capability instead of the beta limit. The required current drive power is between 120MW to 140MW on OpeS.I and is reduced down to 110MW on OpeS.II. Maximum Q value is 6 and 7 on OpeS.I and OpeS.II, respectively.

In concluding the effect of the choice of neutron wall loading, we will summarize the main parameters characterizing the steady state operation capability on T-Ip plane in Figs 16-19 for three different values of neutron wall loading, 0.6MW/m^2, 0.9MW/m^2 and 1.2MW/m^2. The operation space (OpeS.I) is depicted by dashed lines in Figs 17-19. In the case of lower wall loading, the operation space (the minimum plasma current) is bounded by the confinement (power law), and the offset-linear law is not restricting even for the minimum value of wall loading for nuclear testing. As the wall loading is increased, the operation space (minimum plasma current) is then bounded by the beta limit.

For the highest neutron wall loading case of 1.2MW/m^2, the steady state operational region disappears because of the restriction from the beta limit as shown in Fig. 16. Thus, the steady state operation is only achievable with a relatively low neutron wall load.

The required current drive power within the operation space greatly increases as the neutron wall loading is increased, which is attributed to the increase in electron density. Actually, however, the increase of current drive power as the increase of wall loading, is fairly

small, since the reduction of current drive efficiency due to the increase of the density is substantially compensated by the increase of bootstrap fraction due to the increase of beta poloidal as shown in Fig. 18. Thus, the real cause of the increase of current drive power should be the required increase of the operation plasma current for the beta limitation (shift of the operation space toward higher plasma current). Consequently, the steady state operation with higher neutron wall loading, e.g., even with 0.9 MW/m^2, will be difficult due to the requirement of excessively large current drive power.

In Fig.19, the divertor conditions, i.e., peak heat load, are summarized. It is easily seen that the peak heat load is more severe for higher neutron wall loading than for lower one because of larger input power to the divertor region. For the neutron wall loading of $0.6MW/m^2$, peak heat load reduces down to $12MW/m^2$.

The maximum Q-value is achieved at the maximum plasma current of 22MA from the temperature dependency of the contour of equi-Q-value and equi-confinement on the Ip-T plane for each neutron wall loading. In fact, the temperature dependency of equi-Q (Q=const.), equi-confinement (H=const.) and equi-beta (G=const.) are expressed as follows;

$$I_p(Q=\text{const.}) \propto \frac{\langle\sigma v\rangle_0^{1/2}}{T}\frac{f(T)^{1/2}}{1+f_e}T^2 \qquad (3)$$

$$I_p(H=\text{const.}) \propto \frac{T}{\langle\sigma v\rangle_0^{1/2}}\left(1+\frac{f_e+f_I}{2}\right)\frac{1}{f(T)^{1/2}} \qquad (4)$$

$$I_p(G=\text{const.}) \propto \frac{T}{\langle\sigma v\rangle_0^{1/2}}\left(1+\frac{f_e+f_I}{2}\right)\left(1+\frac{\beta_f}{\beta_t}\right)\frac{1}{f(T)^{1/2}} \qquad (5)$$

where $f_e = (n_e-n_{DT})/n_{DT}$, $f_I = n_I/n_{DT}$ (n_e, n_{DT}, n_I are electron, fuel ion and impurity ion density, respectively). β_f and β_t are fast ion and thermal beta values, respectively. $\langle\sigma v\rangle_0$ is the DT fusion reaction rate for uniform density and temperature profiles. The profile effect is expressed by f(T), which is a monotonically decreasing function of temperature. Note that $\langle\sigma v\rangle_0^{1/2}/T$ is almost constant in the range of $8 \leq T \leq 25$ keV. Thus, the increasing nature of Ip(H=const.) and Ip(G=const.) with increasing the temperature arise from the weakly increasing

nature of the functions of $(1+(f_e+f_I)/2)$, $(1+\beta_f/\beta_t)$, $f(T)^{-1/2}$, while Ip(Q=const.) has a slightly stronger temperature dependence as shown by T^2 dependence in Eq. (3). It should also be noted that the contours of I_p(H=const.) and I_p(G=const.) have very similar temperature dependence as can be understood from Eqs (4) and (5). When the temperature becomes further low, I_p(H=const.) and I_p(G=const.) become increasing due to the temperature dependence of $T/<\sigma v>_0^{1/2}$ as shown in Figs 8 and 11.

Fig. 20 shows the operation space in neutron wall loading and temperature plane at the maximum plasma current of 22 MA. The achievable maximum Q-value in steady state operation is about 7 for the neutron wall loading of 0.7MW/m^2, where the energy confinement and current drive power are restricting as shown in Fig. 20. The reduction of the wall loading down to 0.6MW/m^2 substantially relaxes the requirement both for current drive power and divertor condition, though the maximum Q value reduces. When the wall loading is reduced below 0.6MW/m^2, the maximum Q value is then restricted by the contour of equi-enhancement factor for offset-linear confinement scaling law.

IV-2 Possible Extension and Optimization of Steady State Operation Space

IV-2-1 Iron Seeding

It has been proposed to introduce an iron seeding into the plasma edge region for the improvement of long pulse and steady-state operation. It could be expected that the impurity of medium-Z ion species enhances the radiation power loss at the edge region of plasma and, resultantly, reduces the peak heat load on the divertor plate without deteriorating the confinement so much. Fig. 21 and Fig. 22 show the divertor peak heat load on the T-Ip plane for the cases of iron seeding of 0.03% and 0.06%, respectively. The wall loading is 0.8MW/m^2 for both cases. Cooling effect by impurity iron increases proportionally to the square of the plasma density if the concentration fraction is fixed, so that lower temperature and higher density operation is advantageous. However, the lowest operation temperature in the

OpeS I is restricted by beta limit. Even for iron seeding of 0.06%, the divertor peak heat load is about 27MW/m^2. In OpeS II, the divertor peak heat load can be lowered down to about 15MW/m^2. But the current drive power required is 180MW, as shown in Fig. 23 and Q value is only 5 at this operation point. Within a constraint of maximum current drive power of 120MW, there is no available steady-state operation space. Note that the steady-state operation space with no iron seeding shown in Fig. 11 disappears due to the increase of the required heating power to compensate the confinement degradation due to iron seeding.

In these calculations, the radiation loss at the divertor region is assumed to be about 20% of the total input power. In the case of iron seed, this loss may be higher than 20%. If such a remote radiation cooling is taken into account, the divertor peak heat load will further be reduced. Afterwards, the radiation loss at the divertor region is evaluated by using the radiation rate at that region, which is derived from the result of 1D impurity transport simulation with MIST code [8]. The results are shown in Fig. 24 and 25. Fusion power is 500MW for both cases. Fig. 24 shows the operation space with no impurity seeding, while Fig. 25 shows that with iron impurity seeding of 0.05%. The lower boundary of steady state operation region is the contour of equi-enhancement factor of 2 for power law in both cases. The most remarkable difference between these two cases is the reduction of the divertor peak heat load down to about 15MW/m^2 in the impurity seeding case compared with about 20 MW/m^2 in the no seeding case.

The radiation power loss at the plasma edge region is enhanced by the medium-Z impurity seeding, which leads to the reduction of the input power to the divertor region and to the resultant reduction of the divertor peak heat load. However, it can also lead to the deterioration of the plasma confinement at the same time. Therefore, the optimization of the seeding rate to accommodate the requirements from confinement capability and divertor condition is of primary importance.

Some examples of hybrid operation scenarios with iron seeding are presented in Table III and IV. Case 1 in Table III shows the hybrid operation scenario without iron seeding, and the iron seeding is introduced in cases 2 and 3, and the seeding is larger in case 3 (0.07%) than in case 2 (0.03%). In case 1, the divertor peak heat load is not so high (13 MW/m^2) due to rather low operation temperature (11keV),

while, instead, the burn time is only slightly prolonged from the pure inductive burn of 400 seconds in high Q operation mode. As the seeding is increased, the divertor peak heat load is reduced substantially, while the burn time decreases gradually due to the increase of loop voltage with fixed temperature and current drive power. Since the operation temperature is 11 keV, the required enhancement factor is 1.5-1.6 for both power law and offset-linear law. When the operation temperature is increased and the plasma current is decreased, the burn time can be prolonged in the expense of divertor peak heat load and the required enhancement factor. This feature is shown in Table IV, where operation temperature is increased to 13 keV and the plasma current is slightly decreased to 21 MA to prolong the burn time up to ≈ 900 seconds.

IV-2-2 Effect of Higher Magnetic Field

When the fusion power or wall loading is large, the steady state operation space is restricted by the beta limit. In fact, the contour of G=3 is restricting for P_W= 0.8 MW/m^2 (Fig. 11), while the confinement is restricting for P_W= 0.6 MW/m^2 (Fig. 15). It is expected that this restriction can be relaxed, if the TF magnet with slightly higher magnetic field is employed. By this relaxation, the operation space will be expanded to improve the divertor condition by operating with lower temperature.

Fig. 26 shows the operation space, in which the maximum field at the coil is increased to 12.5T from the present design value of 11.5T. The magnetic field at plasma axis increases from 4.85T to 5.32T. As one can see in the figure, the operation space is restricted not by the beta limit but by the confinement requirement. The operation space is thus expanded and the required current drive power is reduced down to about 140MW (Fig. 27). In OpeS II, the steady-state operation becomes possible with the current drive power of 120MW. The divertor heat load is reduced below 30MW/m^2 and 25MW/m^2 at OpeS I and OpeS II, respectively (Fig. 28), because of the reduction of beam power and the increase of operation density and radiation power caused by the increased magnetic field. If higher wall loading, e.g., 0.8MW/m^2, is required for nuclear testing, the increase of the magnetic field is essential.

V. Conclusions

Design point of ITER determined by the previous L-mode scaling laws are examined by the newly developed ITER-L-mode scaling laws, and it is confirmed that the design point has a reasonable ignition capability for the new scaling laws. The present design point is also confirmed to have sufficient ignition capability if evaluated by the newly developed ITER-H-mode scaling laws, though these H-mode scaling laws are based only on the ELM-free H-mode discharges. Scaling laws for ELMy H-mode are now under development, and the evaluation of the ignition capability with these new scaling laws is the next important step in future. Ignition capability is shown to be substantially enlarged when the extension of plasma current and fusion power is achieved.

Characteristics of hybrid long pulse operation scenario are examined. It is shown that, in the hybrid operation with significantly large Q value (Q~30), the available burn time is limited to about 1000 seconds due to rather small current drive power (~30 MW). With increasing the fusion power or wall loading, the available burn time is restricted by the beta limit (G=3) and the maximum burn time is about 4000 seconds for P_f=1.15 GW with full injection of the current drive power (~115 MW). When the wall loading is decreased, the available burn time is restricted by the confinement. Burn time can be fairly prolonged for the operation with the wall loading of, e.g., P_f=0.75 GW, with full power injection. Actually, nearly infinite burn time (steady state) can be expected with this fusion power.

Operation space and the impact of wall loading for steady state operation are studied. As in the hybrid operation scenario, the operation space is restricted by beta limit when the wall loading is high ($P_W \geq 0.6$ MW/m^2). The steady state operation space is fairly narrow, so that the relaxation of the restriction for confinement (e.g., $H \leq 2.1$) and beta (partial pressure of the fast ions is excluded) is essential to obtain the meaningful operation space, though the space is still marginally wide. Even with the above relaxations of the confinement and beta constraints, the steady state operation is shown difficult for higher wall loading due to unacceptably large required current drive power (more than 150 MW is needed for $P_W \geq 0.9$ MW/m^2). Divertor peak heat load is also fairly demanding, especially for the steady state

operation with higher wall loading. In fact, the divertor peak heat load and current drive power are the essential constraints for the steady state operation with higher wall loading. Two possibilities to relax these constraints are presented, i.e., impurity seeding and higher toroidal magnetic field. With the iron seeding of 0.07%, the divertor peak heat load is reduced by a factor of three from the case of no impurity seeding. Higher magnetic field expands the operation space toward the lower plasma current region by relaxing the beta limit. With this expansion, the required current drive power can be reduced substantially, e.g., it is reduced down to 120 MW from 150 MW by increasing the field up to 12.5 T from 11.5 T for P_W = 0.8 MW/m^2. If higher wall loading is needed (e.g., $P_W \geq 0.8$ MW/m^2), higher magnetic field is essential.

Acknowledgements

The authors are grateful to Dr. S. Matsuda for continuous encouragement.

REFERENCES

[1] ITER Physics Team, "ITER Physics",ITER documentation series, N0. 21, IAEA, Vienna (1991).

[2] Cordey, J.G. et al., "A preliminary analysis of the ITER energy confinement H-mode data base", Proceedings of 13th International Conference on Plasma Physics and Controlled Nuclear Fusion Research,Washington, 1990,IAEA-CN-53/F-3-19.

[3] Shimomura, Y., Proceedings of 12th International Conference on Plasma Physics and Controlled Nuclear Fusion Research,Nice, IAEA, Vienna, Vol.3(1988) 273.

[4] Perkins, L.J. et al., "ITER system studies and design space analysis", Proceedings of 13th International Conference on Plasma Physics and Controlled Nuclear Fusion Research,Washington, 1990, ITER-CN-53/F-3-15.

[5] Shimomura, Y., "ITER: Operational Scenario", Proceedings of 13th International Conference on Plasma Physics and Controlled Nuclear Fusion Research,Washington, 1990,IAEA-CN-53/F-2-1.

[6] Naito, O., et al., Nuclear Fusion 30 (1990) 1137.

[7] Harrison, M.M.A., Kukushkin, A., ITER-IL-PH-13-9-E12 (1989).

[8] Cummings, J., Cohen, S., Hulse, R., Redi, M., ITER-IL-PH-13-9-U-25 (1989).

Acknowledgements

The authors are grateful to Dr. S. Matsuda for continuous encouragement.

REFERENCES

[1] ITER Physics Team, "ITER Physics",ITER documentation series, N0. 21, IAEA, Vienna (1991).

[2] Cordey, J.G. et al., "A preliminary analysis of the ITER energy confinement H-mode data base", Proceedings of 13th International Conference on Plasma Physics and Controlled Nuclear Fusion Research,Washington, 1990,IAEA-CN-53/F-3-19.

[3] Shimomura, Y., Proceedings of 12th International Conference on Plasma Physics and Controlled Nuclear Fusion Research,Nice, IAEA, Vienna, Vol.3(1988) 273.

[4] Perkins, L.J. et al., "ITER system studies and design space analysis", Proceedings of 13th International Conference on Plasma Physics and Controlled Nuclear Fusion Research,Washington, 1990, ITER-CN-53/F-3-15.

[5] Shimomura, Y., "ITER: Operational Scenario", Proceedings of 13th International Conference on Plasma Physics and Controlled Nuclear Fusion Research,Washington, 1990,IAEA-CN-53/F-2-1.

[6] Naito, O., et al., Nuclear Fusion 30 (1990) 1137.

[7] Harrison, M.M.A., Kukushkin, A., ITER-IL-PH-13-9-E12 (1989).

[8] Cummings, J., Cohen, S., Hulse, R., Redi, M., ITER-IL-PH-13-9-U-25 (1989).

Table I Typical plasma parameters for reference ignition operation

Plasma current	(MA)	22.0
Herium concentration	n_α/n_e	0.1
Neutron wall load	(MW/m^2)	1.0
Burn time	(s)	400
Loop Voltage	(V)	0.115
Effective charge	Z_{eff}	1.66
Bootstrap current fraction	I_{BS}/Ip	0.14
Safety factor	$q_\psi(95\%)$	3.0
Troyon factor	g	1.99
Toroidal beta	(%)	4.2
Poloidal beta		0.65
Electron density	$n_e(10^{20}m^{-3})$	1.22
Electron temperature	Te(keV)	10.0
Required energy confinement time	τ_E (s)	3.8
Required fusion product	$n_{DT}(0)\tau_E Ti(0)$ (10^{21}keV s m^{-3})	8.5
Enhancement factor	H_{IP}/H_{IO}	2.0/2.0
Enhancement factor	H_G/H_{SO}	1.9/1.9
Fusion power	(MW)	1080
Radiation loss from main	(MW)	67
Radiation loss from edge	(MW)	35
Divertor peak power load	(MW/m^2)	(8.5)
Divertor peak temperature	(eV)	(28)

Table II Examples of plasma parameters for hybrid long pulse and high Q operations.

	Inductive Ignition	Hybrid High-Q	Hybrid Long pulse
Ip (MA)	22	20	15.4
Neutron wall load (MW/m^2)	1	0.9	0.8
Q	-	30	7.9
Burn time (s)	400	870	2500
I_{BS}/Ip	0.14	0.18	0.3
I_{CD}/Ip	0	0.08	0.3
Loop voltage (V)	0.12	0.07	0.045
Z_{eff}	1.66	1.74	2.2*
$q_\psi(95\%)$	3	3.3	4.4
g-Troyon	2.0	2.2	2.7
beta (%)	4.2	4.3	4.0
beta-p	0.62	0.8	1.4
n_e ($10^{20}m^{-3}$)	1.22	1.0	1.06
Te (keV)	10	12	11
τ_E (s)	3.84	3.14	2.66
H_{IP}	2.0	2.0	2.2
H_{IO}	2.0	1.8	1.8
H_{IP} (H-mode)	0.69	0.67	0.76
H_{IO} (H-mode)	0.77	0.73	0.85
PFusion (MW)	1080	1000	860
P_{CD} (MW)	0	33	110
Prad,main (MW)	67	55	90
Prad,edge (MW)	35	31	95
P_{div} (MW)	45	60	40

H_{IP}: enhancement factor of energy confinement from ITER Power Law Scaling of L-mode

H_{IO}: enhancement factor of energy confinement from ITER Off-set Linear Scaling

Pdiv: power flow into one outer divertor channel

H_e: 10%

*n_{Fe}/n_e=0.0007

Table III Examples of plasma parameters as well as divertor peak heat load with iron impurity seeding for moderate burn time (around 500 seconds) hybrid operation.

	case 1	case 2	case 3
Ip (MA)	22	←	←
Neutron wall load (MW/m^2)	0.8	←	←
Q	10	←	←
Burn time (s)	560	500	450
I_{BS}/Ip	0.14	0.14	0.14
I_{CD}/Ip	0.18	0.18	0.18
Loop voltage (V)	0.082	0.091	0.103
Z_{eff}	1.73	1.92*	2.2**
q (95%)	3	←	←
g-Troyon	1.93	1.93	1.95
beta (%)	4.1	4.1	4.1
beta-p	0.65	0.65	0.65
n_e ($10^{20}m^{-3}$)	1.01	1.02	1.04
Te (keV)	11	←	←
τ_{E} (s)	2.49	2.67	2.97
H_{IP}	1.57	1.64	1.74
H_{IO}	1.42	1.51	1.65
τ_EH-mode (IP) (s)	4.59	4.74	4.98
τ_EH-mode (IO) (s)	4.40	4.48	4.63
P_{Fusion} (MW)	880	←	←
P_{CD} (MW)	87	←	←
P_{core} (MW	55	68	87
P_{edge}(MW)	31	55	90
P_{div} (MW/m^2)	13.0	9.8	4.7
T_{div} (eV)	45	31	11

Pdiv: divertor heat load

T_{div}: divertor temperature

H_e: 10%

*nFe/n_e=0.0003

**nFe/n_e=0.0007

Table IV Examples of plasma parameters as well as divertor peak heat load with iron impurity seeding for long burn time (around 1000 seconds) hybrid operation.

	case 1	case 2	case 3
Ip (MA)	21	←	←
Neutron wall load (MW/m^2)	0.8	←	←
Q	10	←	←
Burn time (s)	950	890	850
I_{BS}/Ip	0.16	0.16	0.16
I_{CD}/Ip	0.25	0.25	0.24
Loop voltage (V)	0.060	0.064	0.067
Zeff	2.01*	2.13**	2.26***
q (95%)	3.17	←	←
g-Troyon	2.15	2.15	2.15
beta (%)	4.3	4.6	4.7
beta-p	0.75	0.75	0.76
n_e ($10^{20}m^{-3}$)	0.89	0.89	0.90
Te (keV)	13	←	←
τ_E (s)	2.63	2.73	2.83
HIP	1.74	1.77	1.81
HIO	1.55	1.60	1.66
τ_EH-mode (IP) (s)	4.40	4.47	4.55
τ_EH-mode (IO) (s)	4.21	4.25	4.30
PFusion (MW)	875	←	←
PCD (MW)	87	←	←
Pcore (MW	59	65	72
Pedge(MW)	46	58	69
P_{div} (MW/m^2)	12.3	10.4	8.5
T_{div} (eV)	47	40	32

P_{div}: divertor heat load
T_{div}: divertor temperature
H_e: 10%
*nFe/n_e=0.0003
**nFe/n_e=0.0005
***nFe/n_e=0.0007

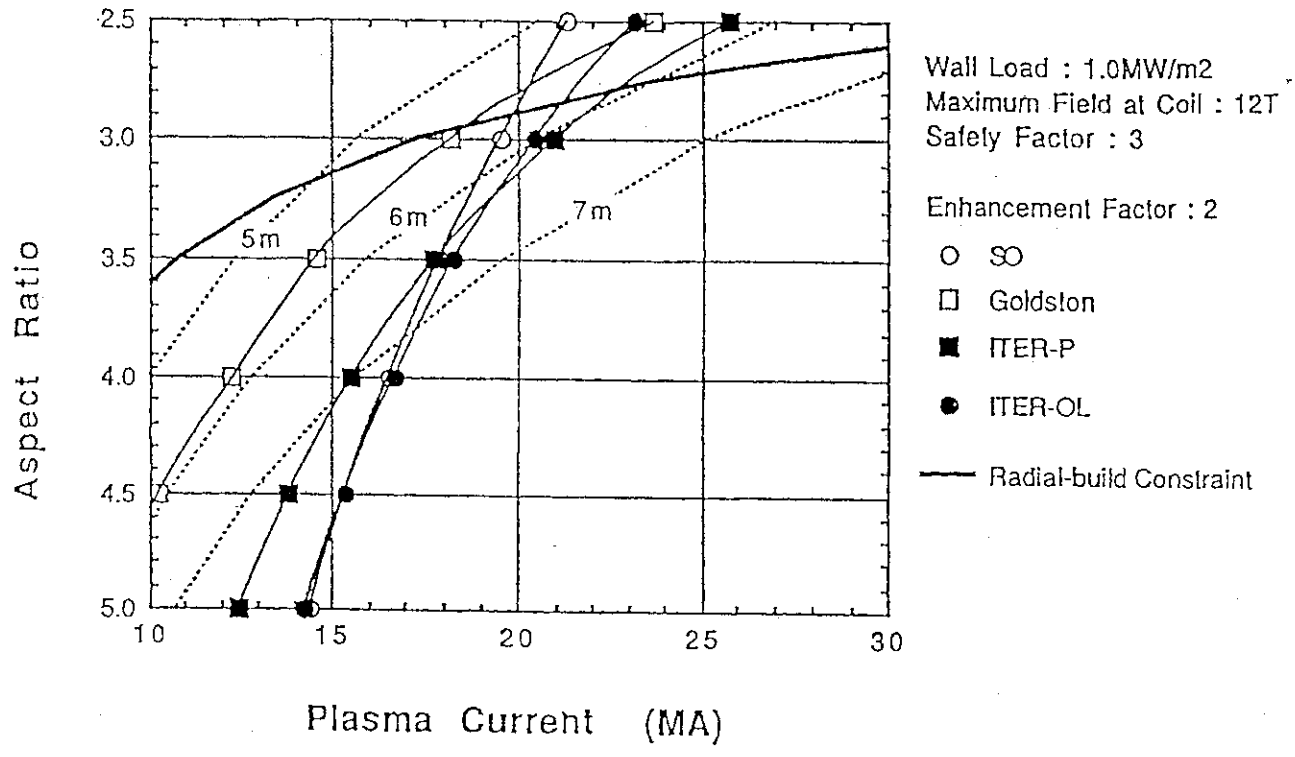

Fig. 1 Contours of equi-enhancement factor (H=2) for various L-mode confinement scalings (SO: Shimomura-Odajima, Goldston, ITER-P: ITER L power law, ITER-OL: ITER L offset-linear) to achieve the ignition on the Aspect ratio - Plasma current (A-I) space. Wall loading is assumed $Pw=1MW/m^2$. Thick solid line and dotted lines are radial build constraint for 400 seconds of inductive burn and the contours of equi-major radius, respectively, which are evaluated by the constraints of the safety factor ($q\psi=3$ and maximum field at TF coil ($B_{max}=12T$).

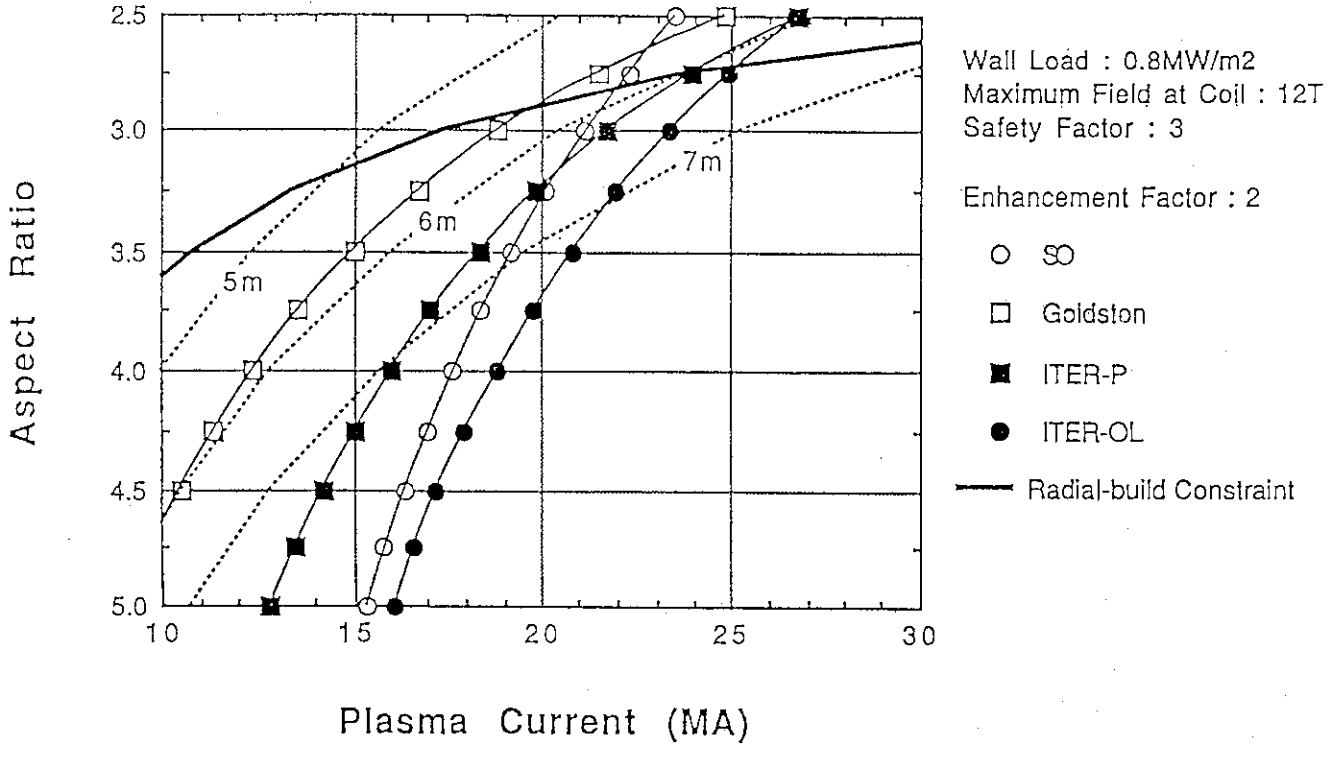

Fig. 2 Same as Fig. 1 for the case of $Pw=0.8MW/m^2$.

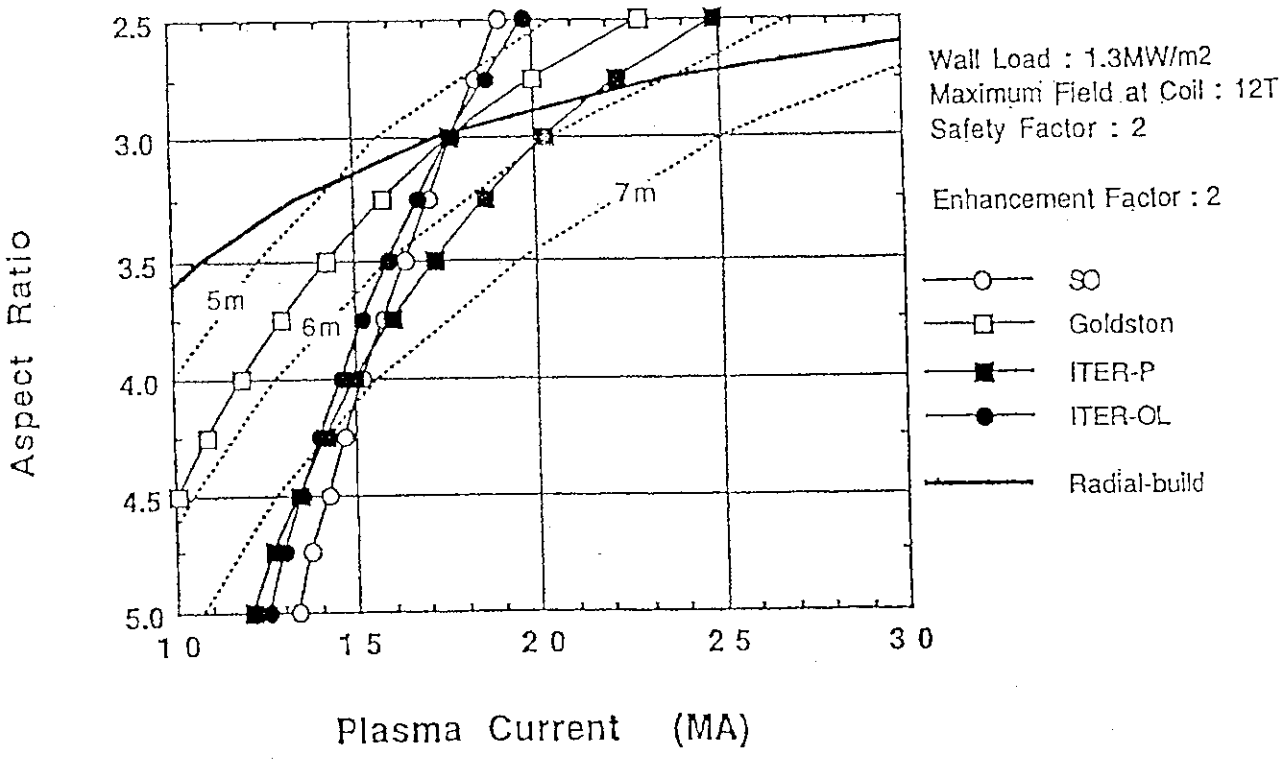

Fig. 3 Contours of equi-enhancement factor (H=2) for various L-mode confinement scalings (SO: Shimomura-Odajima, Goldston, ITER-P: ITER L power law, ITER-OL: ITER L offset-linear) to achieve the ignition on the Aspect ratio - Plasma current (A-I) space. Wall loading is assumed Pw=1.3MW/m^2. Thick solid line and dotted lines are radial build constraint for 400 seconds of inductive burn and the contours of equi-major radius, respectively, which are evaluated by the constraints of the safety factor (qψ=3 and maximum field at TF coil (B_{max}=12T).

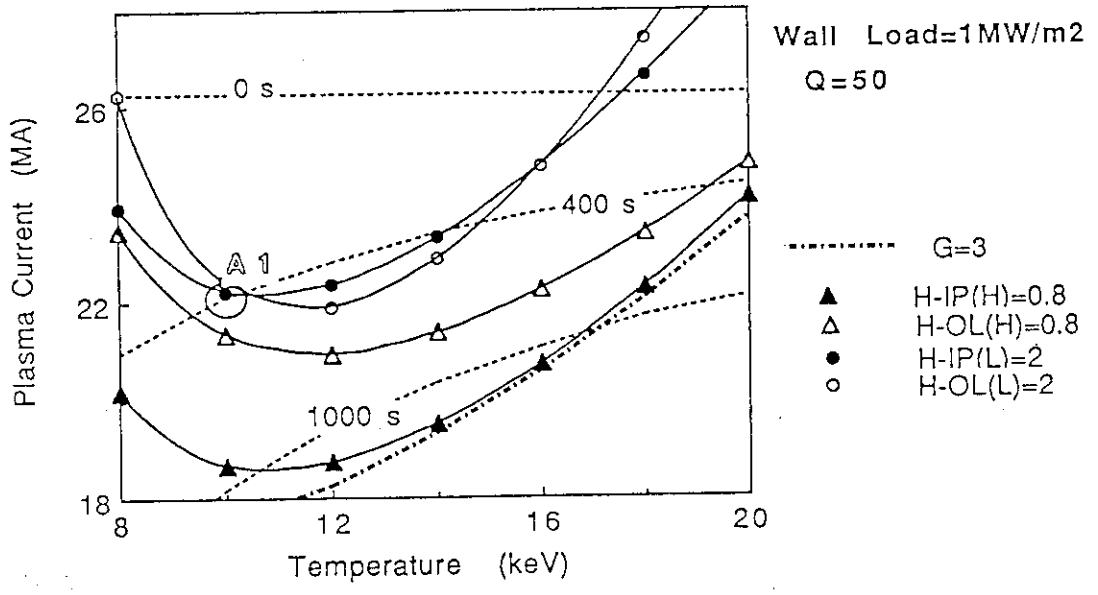

Fig. 4 Contour of equi-Q (Q=50) lines for various L-mode (ITER-P and ITER-OL) and H-mode (ITER-P and ITER-OL) scaling laws on plasma temperature and plasma current (T-Ip) space. Dotted lines show the contours of equi-burn time.

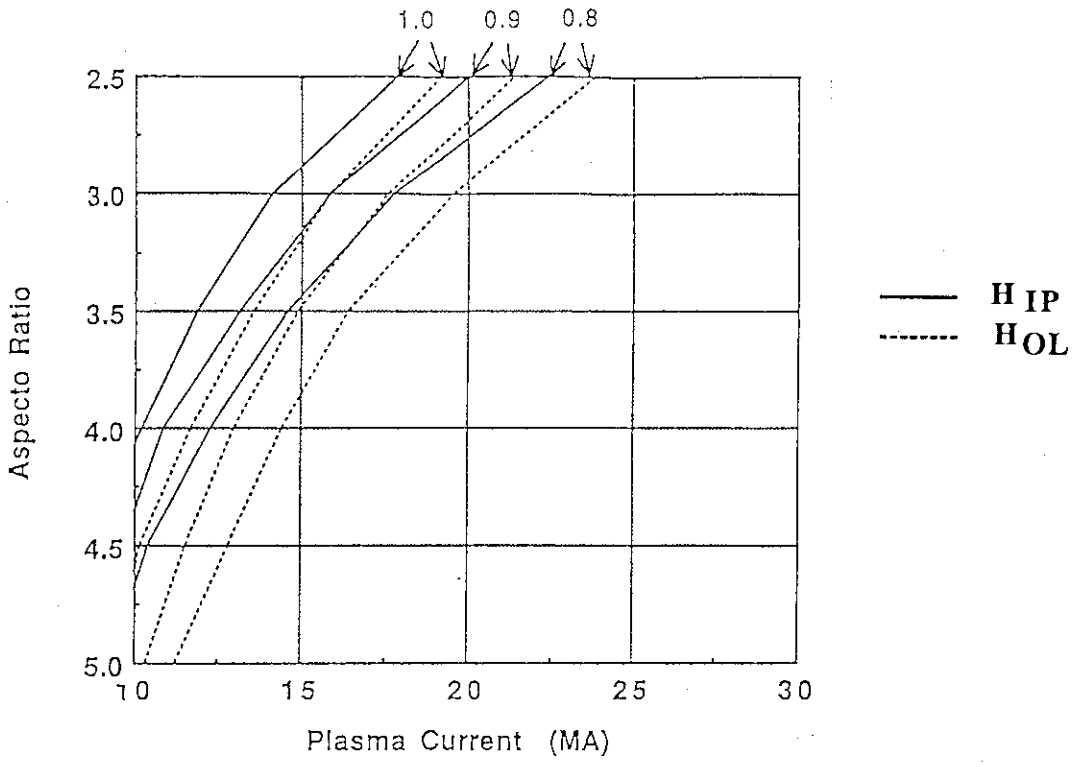

Fig. 5 Contours of equi-enhancement factor (H=1, 0.9 and 0.8) for typical H-mode confinement scalings (ITER-H-P: ITER H power law, ITER-H-OL: ITER H offset-linear) to achieve the ignition on the Aspect ratio - Plasma current (A-I) space. Wall loading is assumed Pw=1MW/m^2.

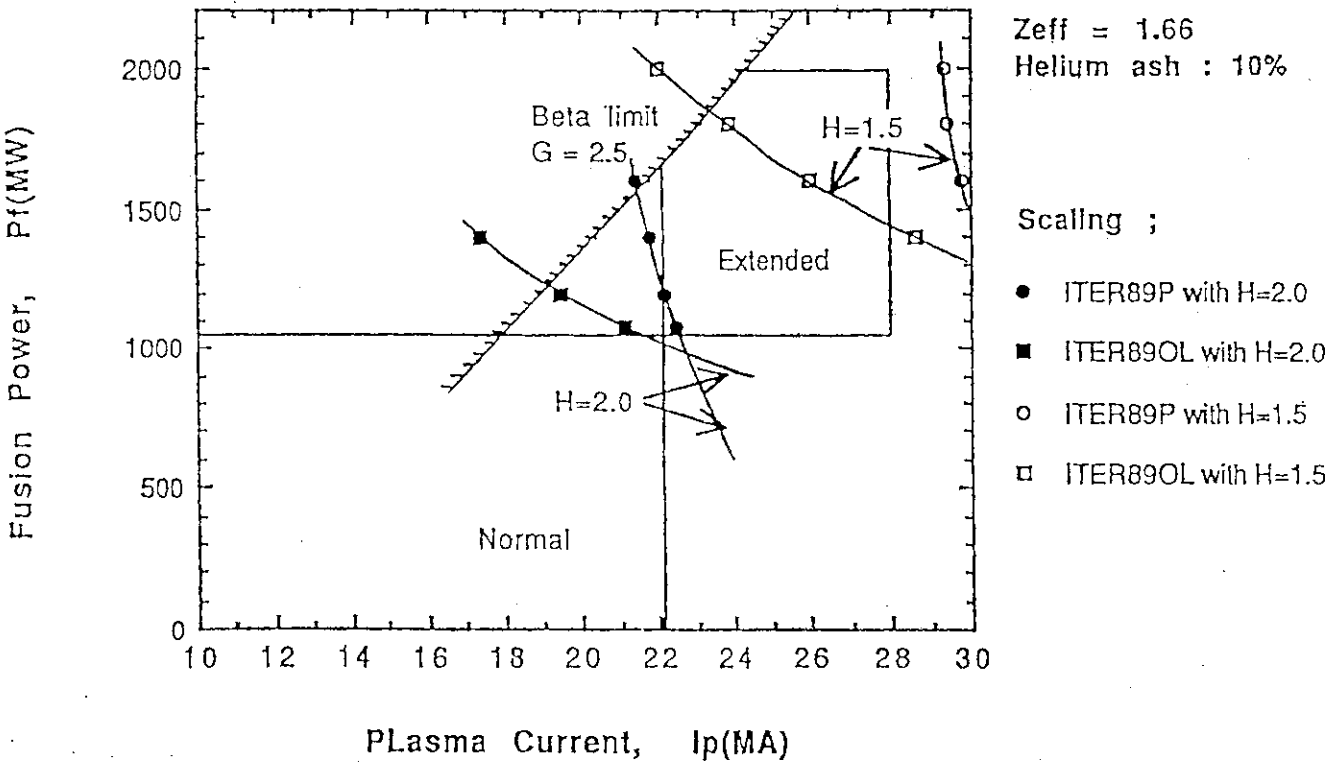

Fig. 6 Ignition performance by extended operation on plasma current and fusion power space. Contours of equi-enhancement factor (H=2 and 1.5) for power and offset-linear L-mode scaling laws are depicted on the space. Constraint of beta limit (G=2.5) is also shown. Other important assumptions are that Zeff=1.66 and helium concentration is 10%.

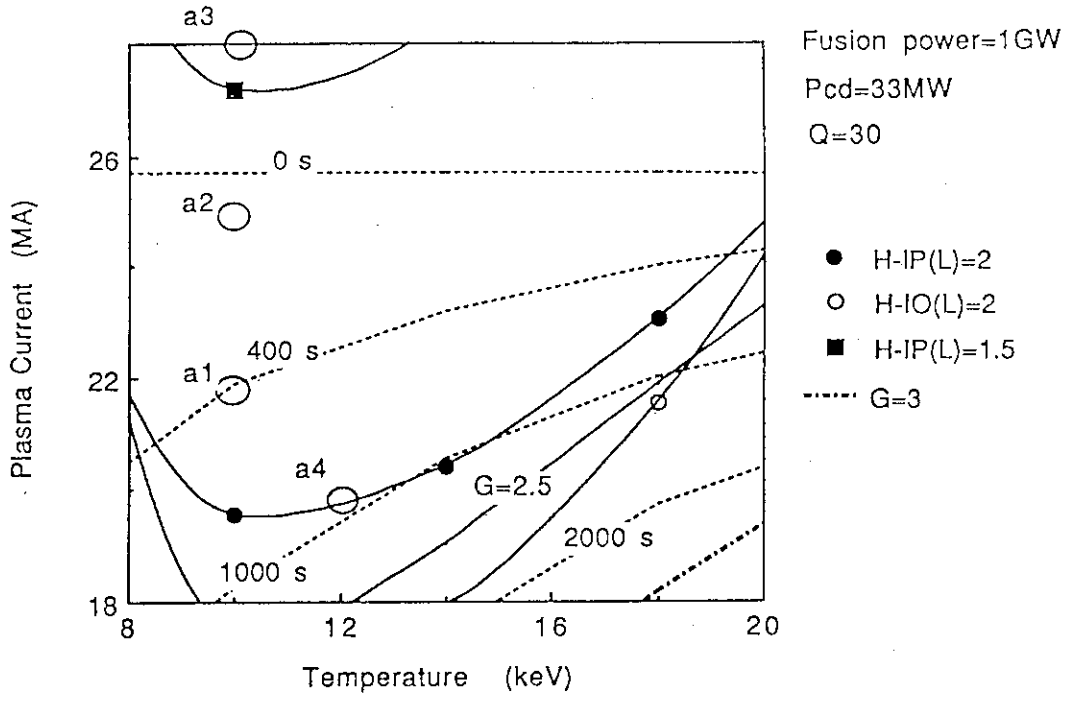

Fig. 7 Contours of equi-enhancement factor for various L-mode scaling laws to achieve high Q (Q=30) performance on T-Ip space in the case of P_f=1GW. Dotted lines show contours of equi-burn time.

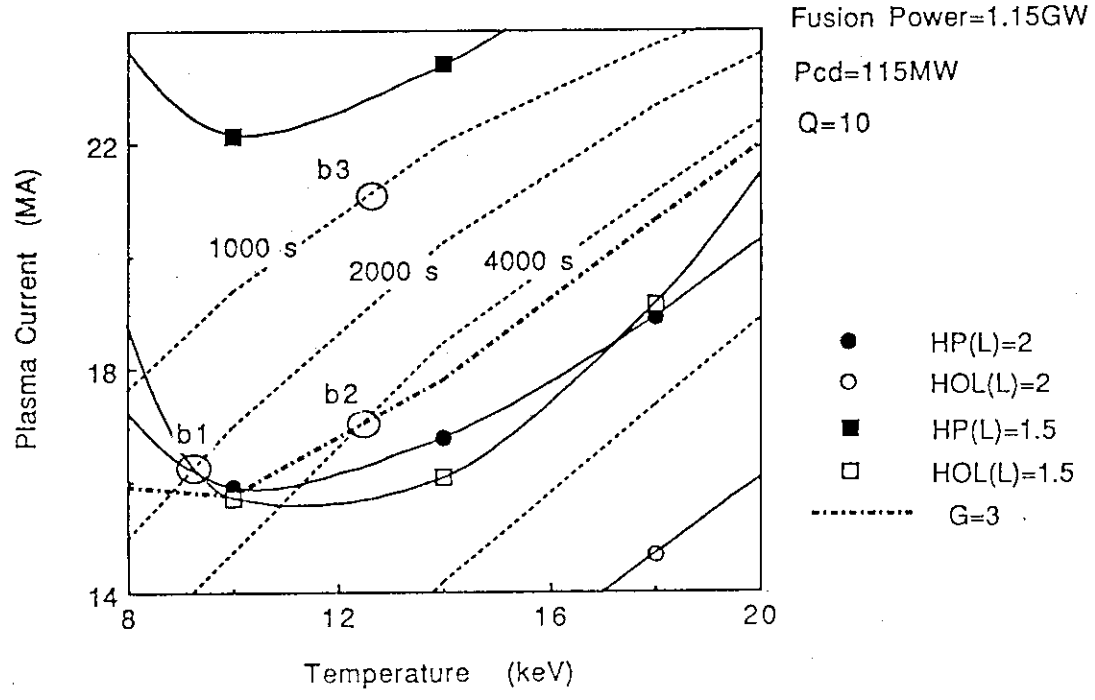

Fig. 8 Same as Fig. 7 for higher fusion power (P_f=1.15GW) with full power injection (P_{cd}=115MW) to prolong burn time by hybrid operation.

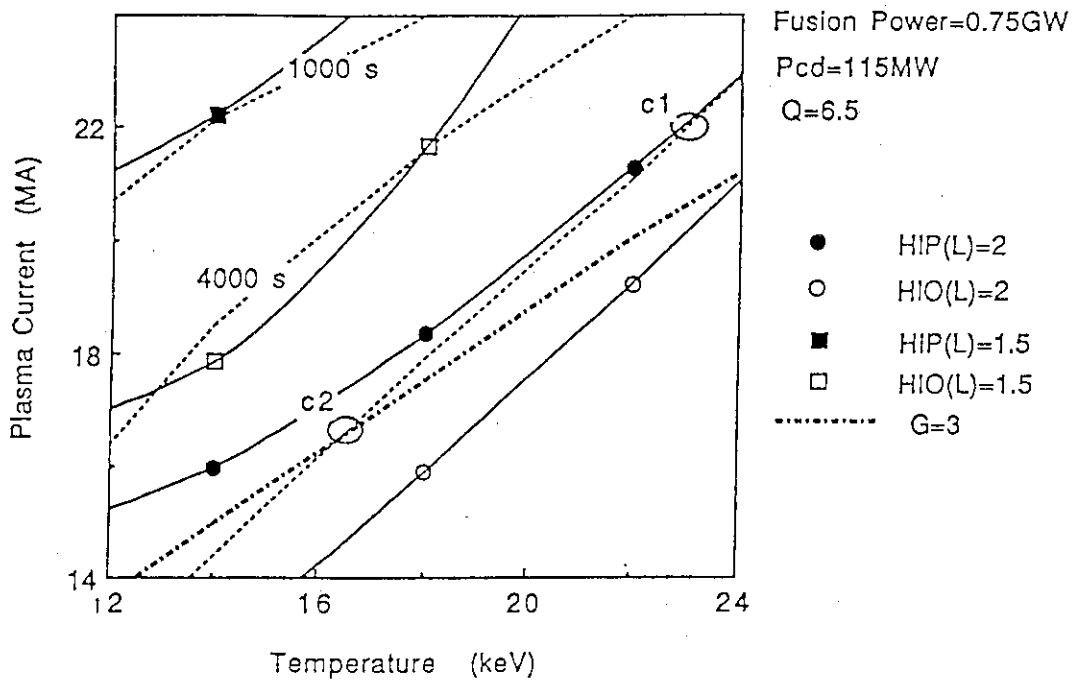

Fig. 9 Same as Fig. 8 for lower fusion power (P_f=0.75GW) with full power injection (P_{cd}=115MW) to prolong burn time still further by hybrid operation.

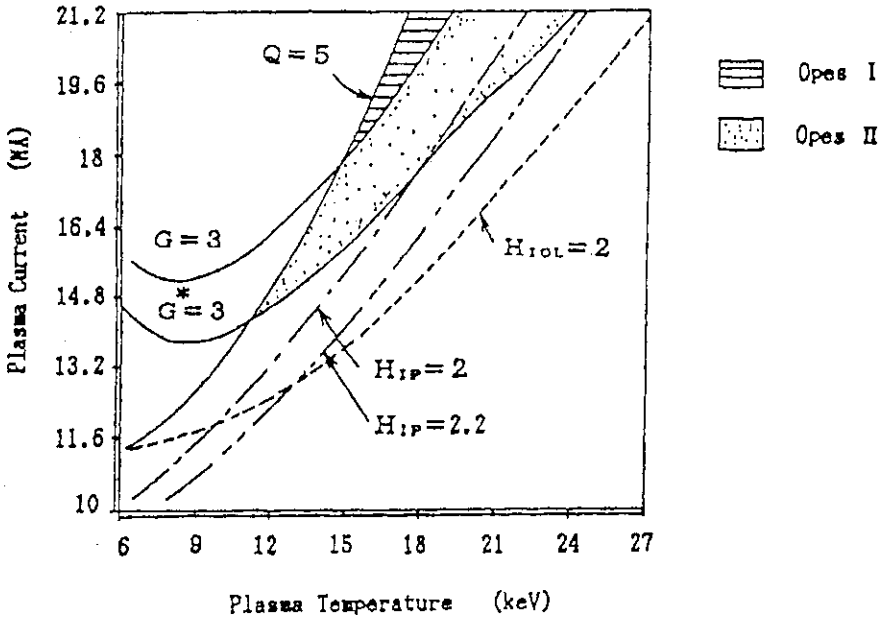

Fig. 11 Operation space on T-Ip plane for steady state operation with wall loading of 0.8MW/m^2. Operation space I (Opes I) is restricted by Q=5 (equivalently current drive power) and beta limit (G=3). Operation space II (Opes II) is restricted by Q=5 and rather optimistic beta limit (Troyon coefficient including only partial pressure of fast ions G^*=3). Rather optimistic confinement restriction (H=2.1) is also employed, which bounds the operation space in high temperature region (T.18 keV).

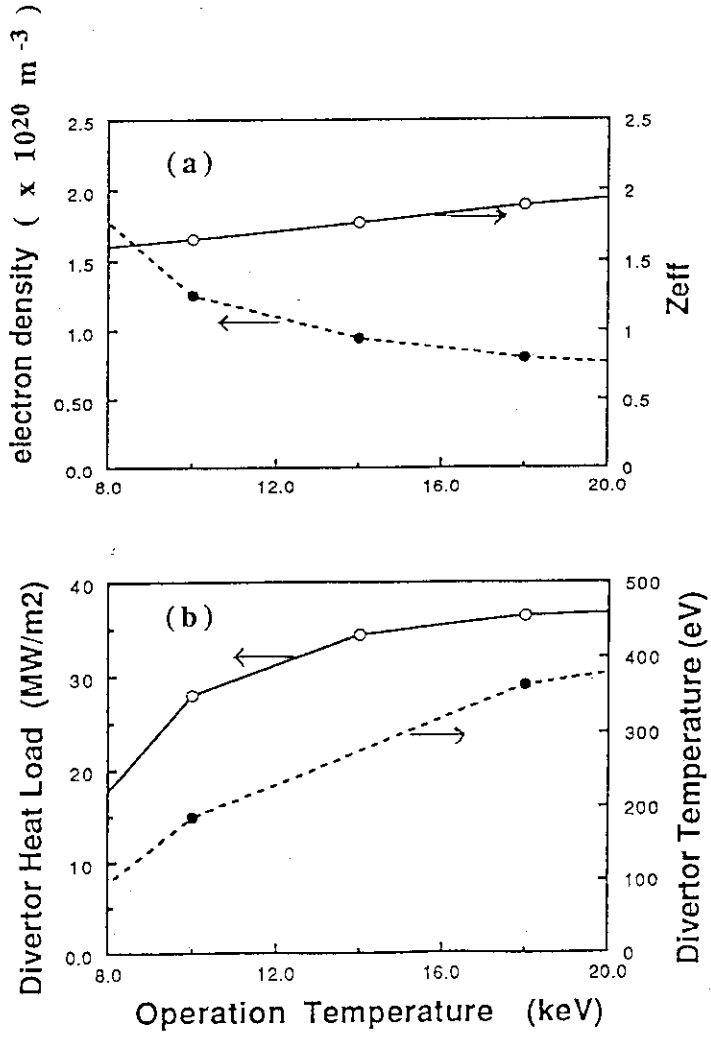

Fig. 10 (a) Typical plasma parameters (electron density and Zeff) for various operation points of Fig. 8. Operation points are chosen along the beta restriction for high temperature region (T>10 keV) and along the confinement restriction for lower temperature (T<10 keV).
(b) Divertor peak heat load and temperature for the operation points of (a).

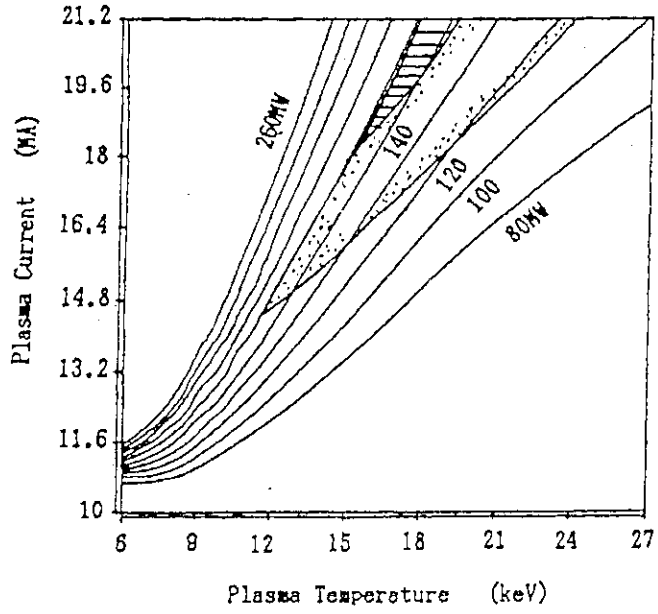

Fig. 12 Contours of equi-required current drive power for steady state operation with wall loading of 0.8 MW/m^2.

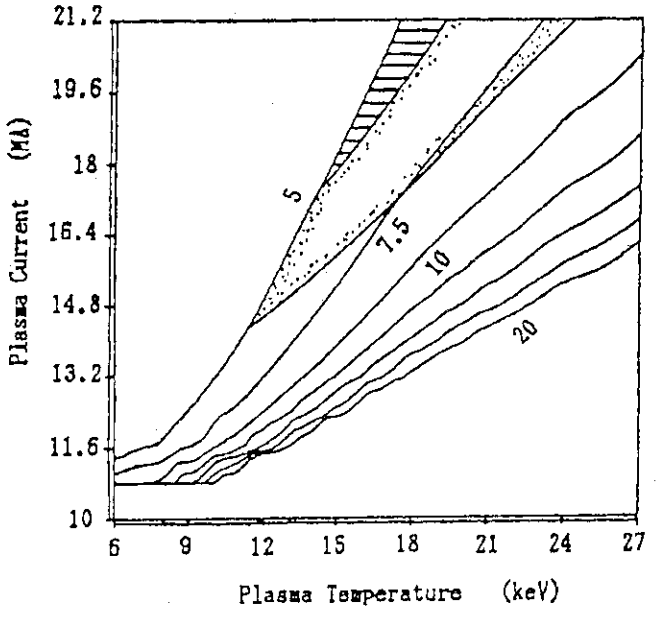

Fig. 13 Contours of equi-Q value for steady state operation with wall loading of 0.8 MW/m^2.

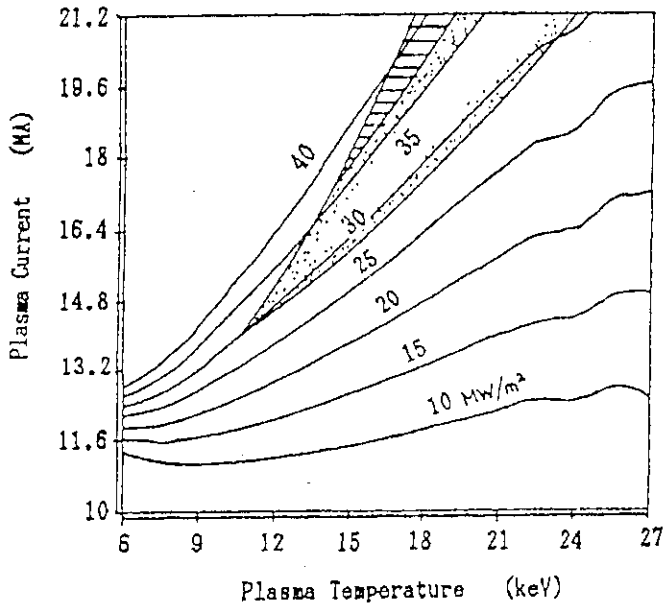

Fig. 14 Contours of equi-peak heat load on divertor plate for steady state operation with wall loading of 0.8 MW/m^2.

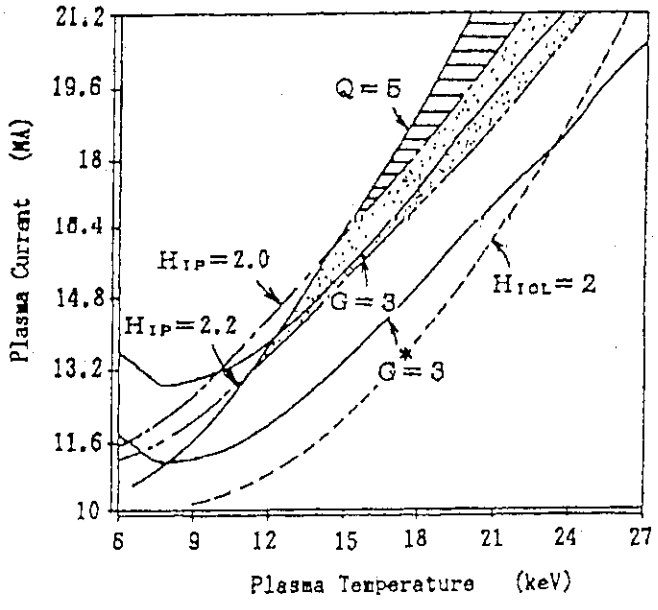

Fig. 15 Operation space on T-Ip plane for steady state operation with wall loading of 0.6 MW/m^2. Operation space I (Opes I) is restricted by Q=5 (equivalently current drive power), confinement (H_{IP}=2). Operation space II (Opes II) is restricted by Q=5 and rather optimistic restriction (H_{IP}=2.2).

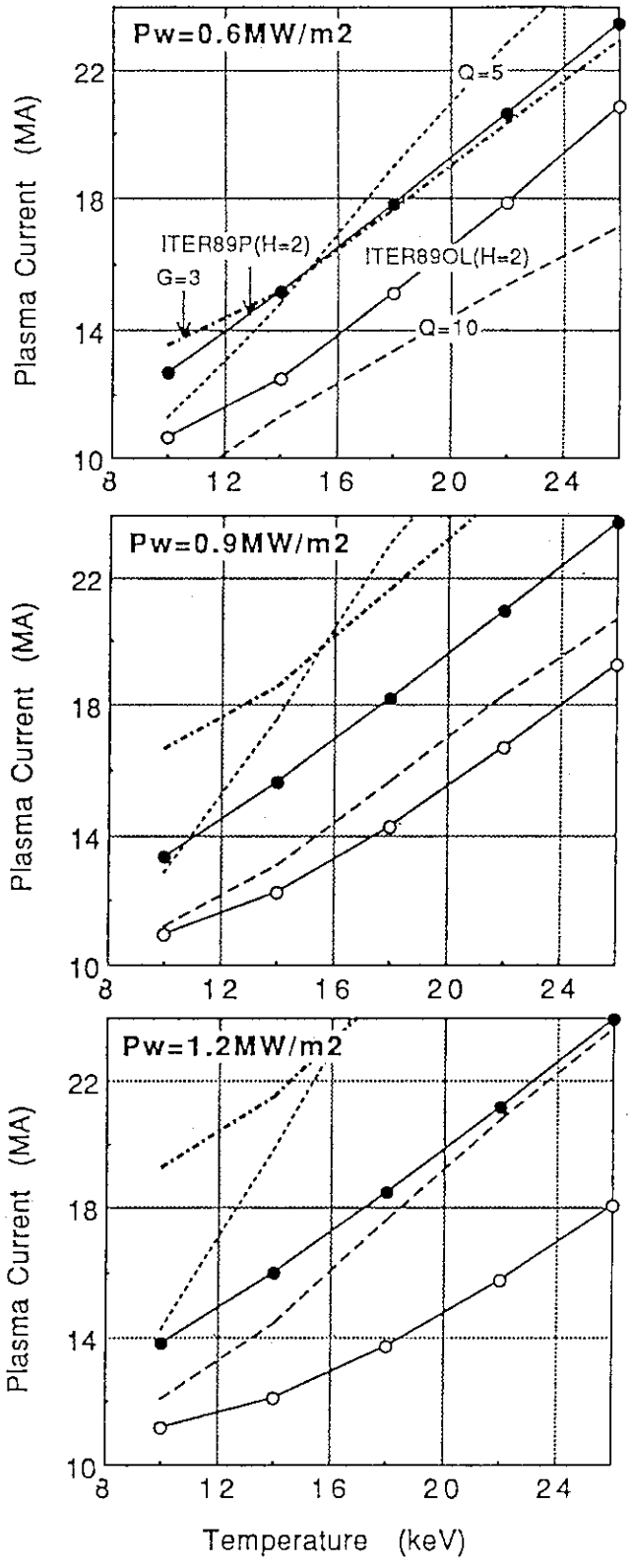

Fig. 16 Operation space for steady state operation with various values of wall loading, (a) 0.6 MW/m^2, (b) 0.9 MW/m^2, (c) 1.2 MW/m^2 on T-Ip space. When the wall loading becomes higher, restriction of beta (G=3) becomes predominant. Resultantly, the available operation space within maximum plasma current of 22 MA almost disappears.

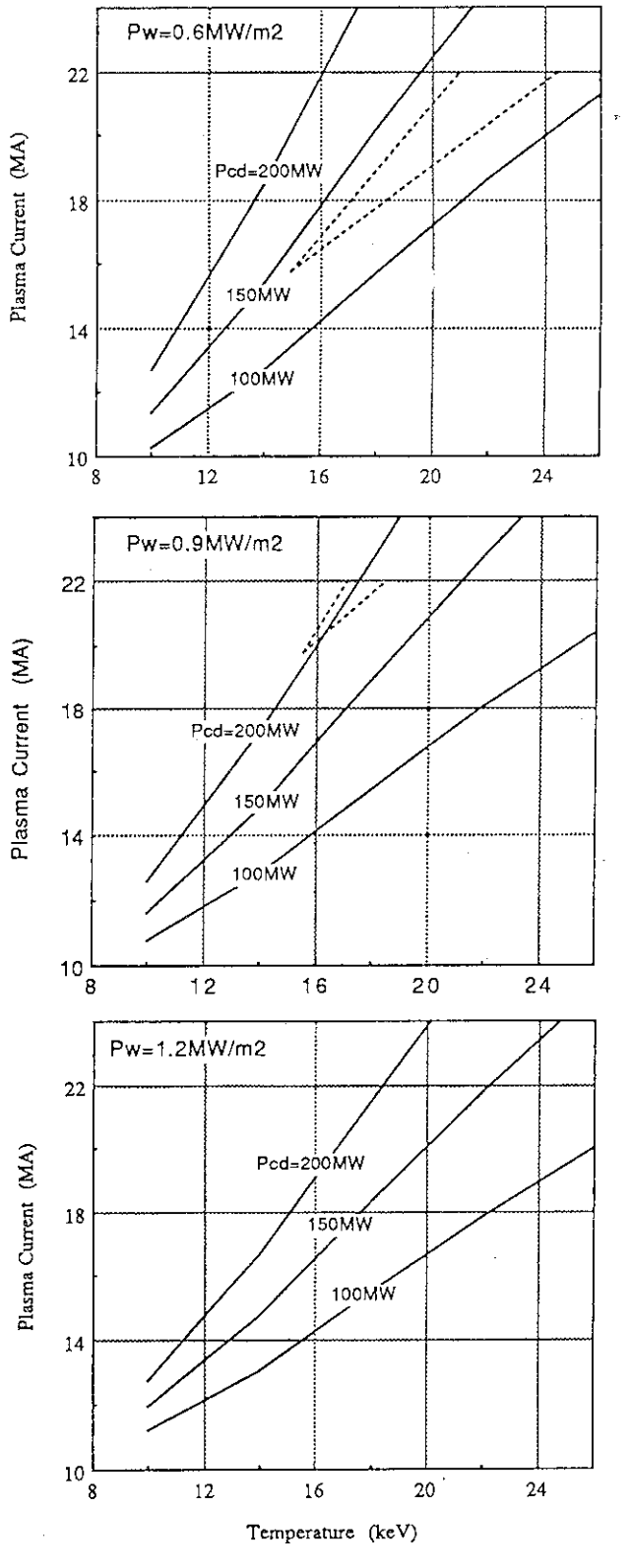

Fig. 17 Contours of equi-required current drive power on the operation space of Fig. 16. When the wall loading is higher than 0.9 MW/m^2, required current drive power is around 200 MW or more, so that, actually, these operations cannot be achieved.

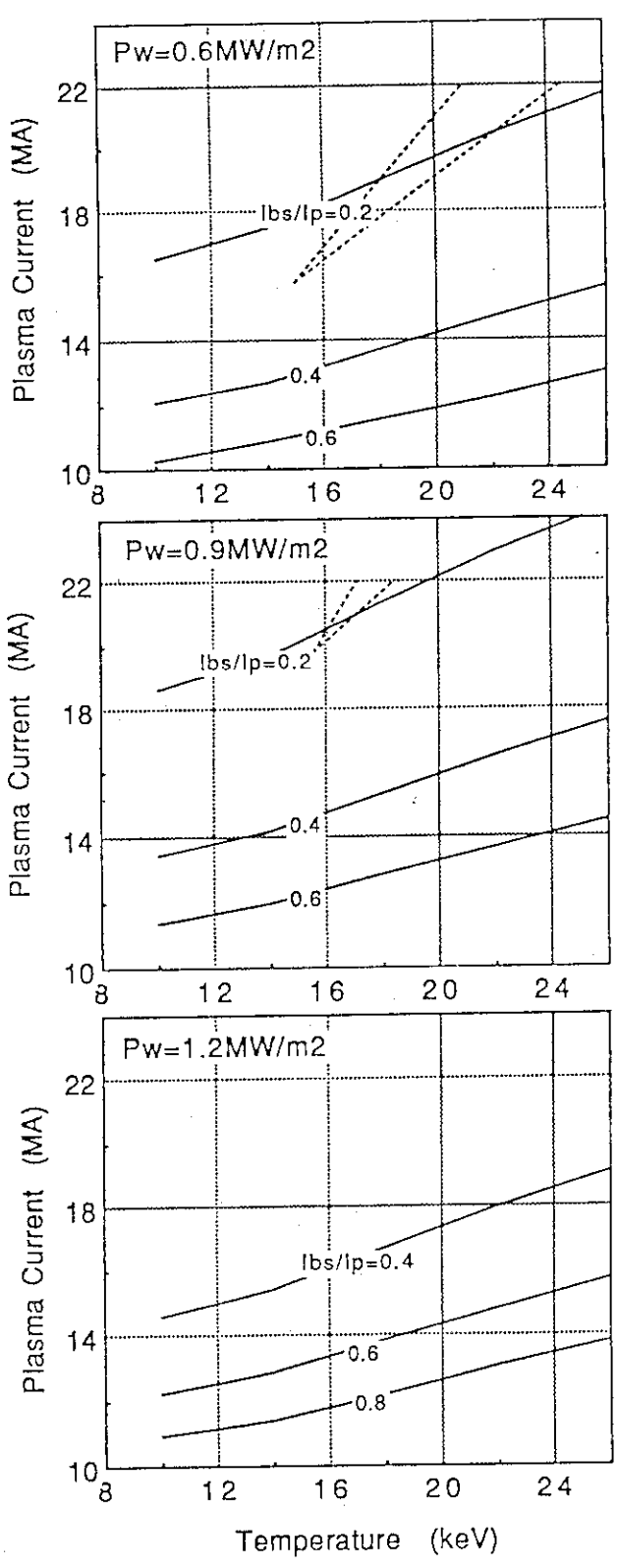

Fig. 18 Contours of equi-bootstrap current fraction on the operation space of Fig. 16. Maximum available bootstrap fraction is about 30% for the wall loading of 0.6 MW/m^2.

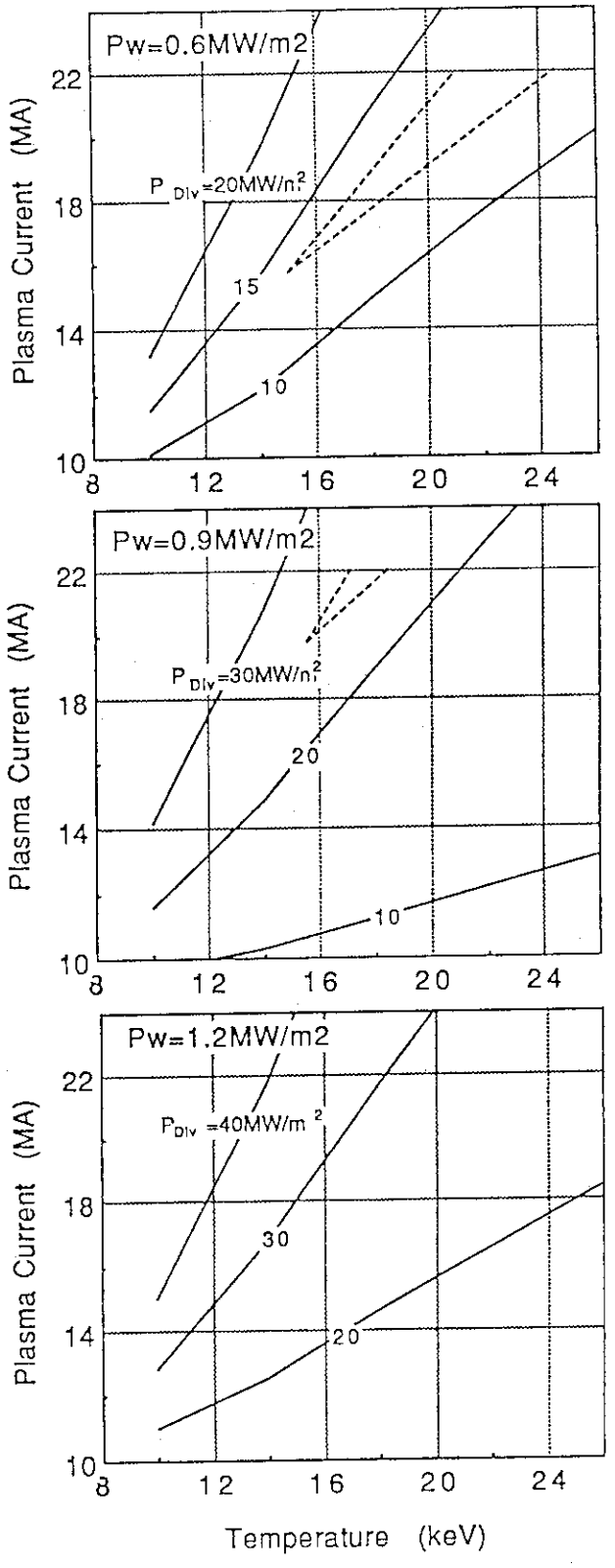

Fig. 19 Contours of equi-peak heat load on the divertor plate on the operation space of Fig. 16. Even for the wall loading of 0.6 MW/m^2, peak heat load is larger than 10 MW/m^2. When the wall loading is higher, peak heat load becomes prohibitively large.

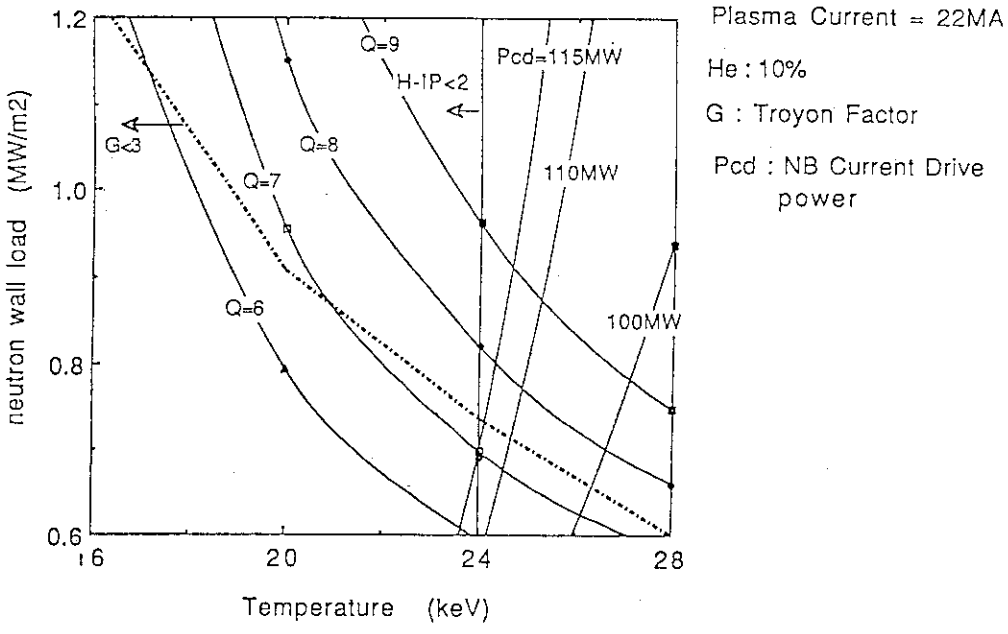

Fig. 20 Contours of equi-Q value for the steady state operation on the temperature and neutron wall loading plane. Contours of equi-required current drive power is also shown. When the operation is restricted by the confinement (H_{IP}<2), beta (G<3) and current drive power (P_{cd}<115 MW), the available wall loading is about 0.7 MW/m^2.

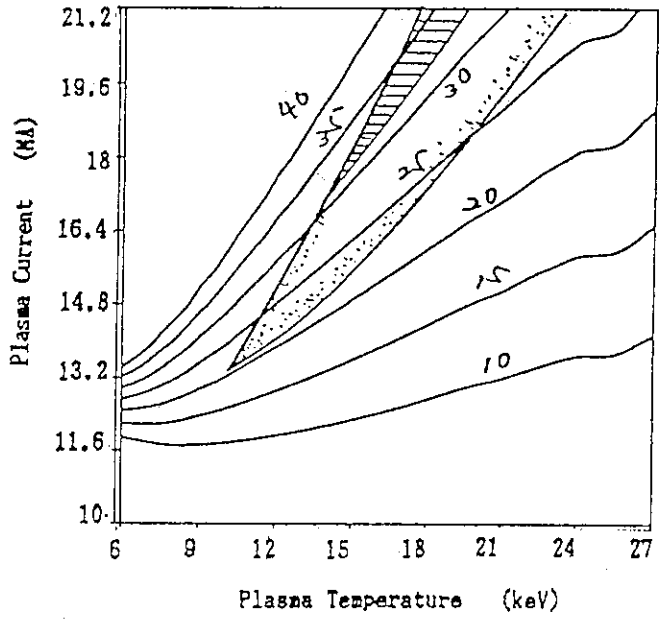

Fig. 21 Contours of equi-peak heat load on divertor plate on the T-Ip operation space for steady state operation with 0.03% of iron seeding.

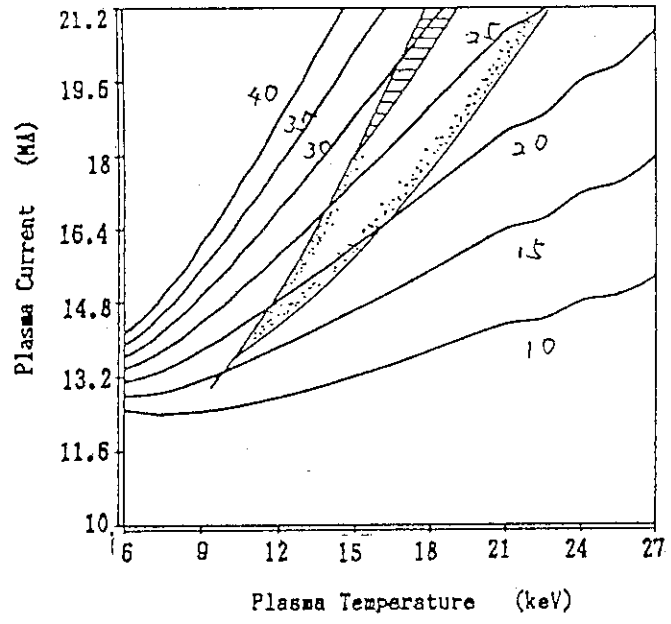

Fig. 22 Contours of equi-peak heat load on divertor plate on the T-Ip operation space for steady state operation with 0.06% of iron seeding.

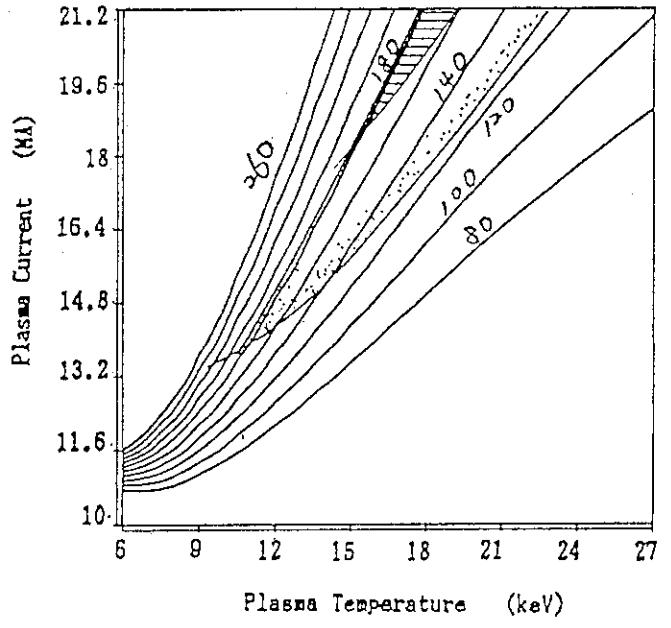

Fig. 23 Contours of equi-required current drive power on the T-Ip operation space for steady state operation with 0.06% of iron seeding.

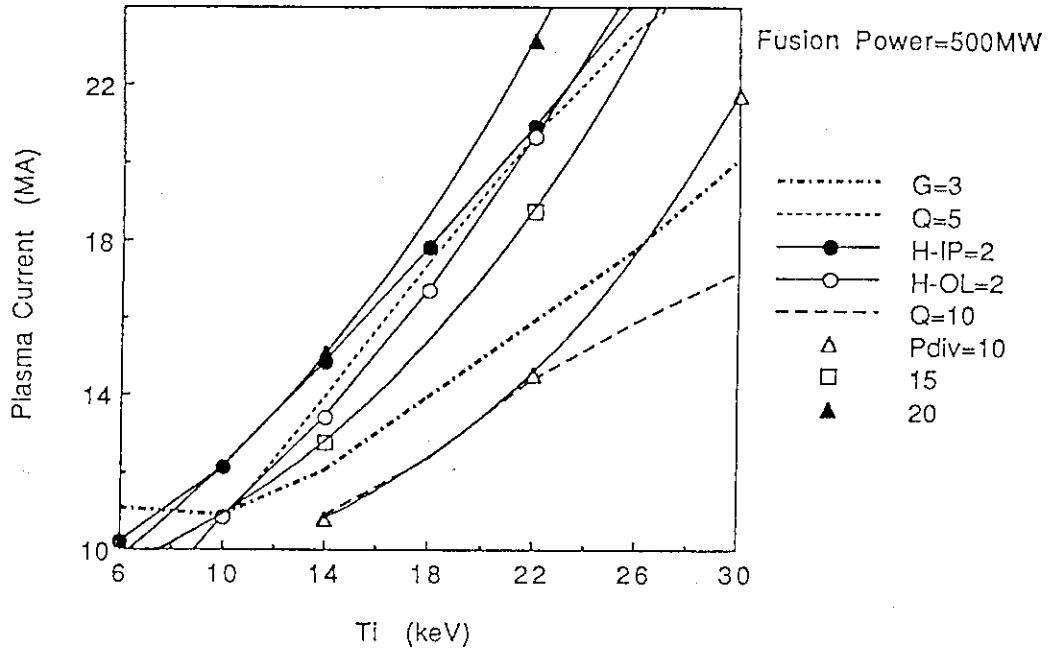

Fig. 24 Steady state operation space on T-Ip plane for 500 MW of fusion power with no iron seeding. Contours of equi-peak heat load on divertor plate are depicted on the operation space bounded by power law confinement restriction.

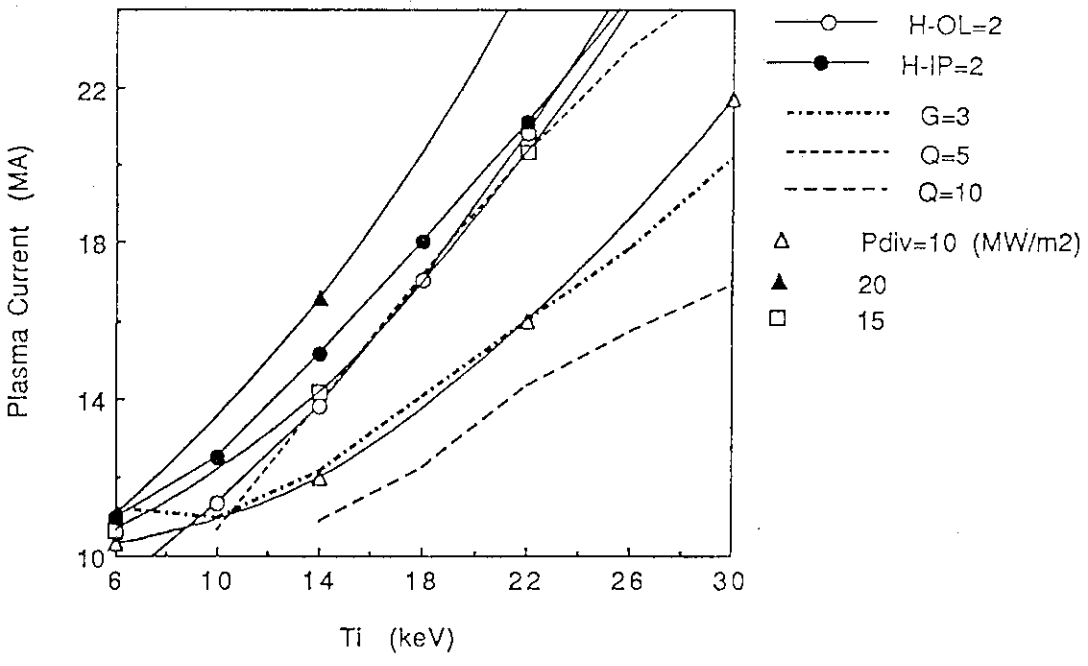

Fig. 25 Steady state operation space on T-Ip plane for 500 MW of fusion power with 0.05% of iron seeding. Contours of equi-peak heat load on divertor plate are depicted on the operation space bounded by power law confinement restriction.

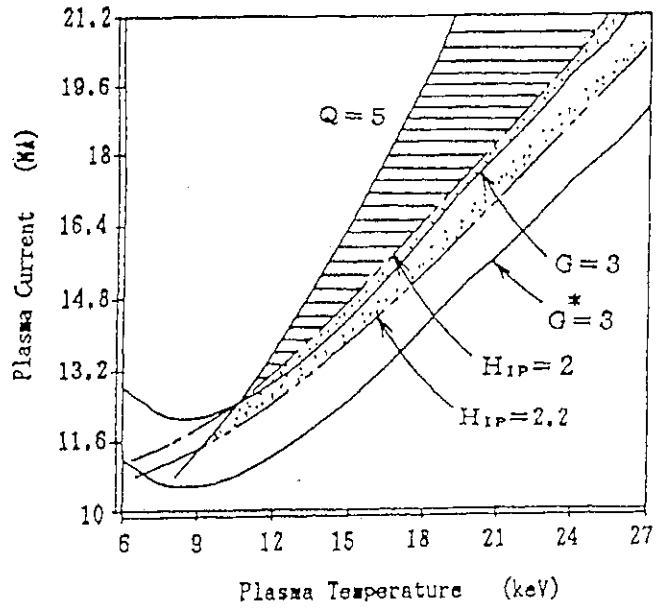

Fig. 26 Operation space on T-Ip plane for steady state operation with wall loading of 0.8 MW/m^2 for the case of increased toroidal magnetic field (B_{max}=12.5 from 11.5 T). The operation space is bounded by the confinement restriction, instead of beta, due to increased field.

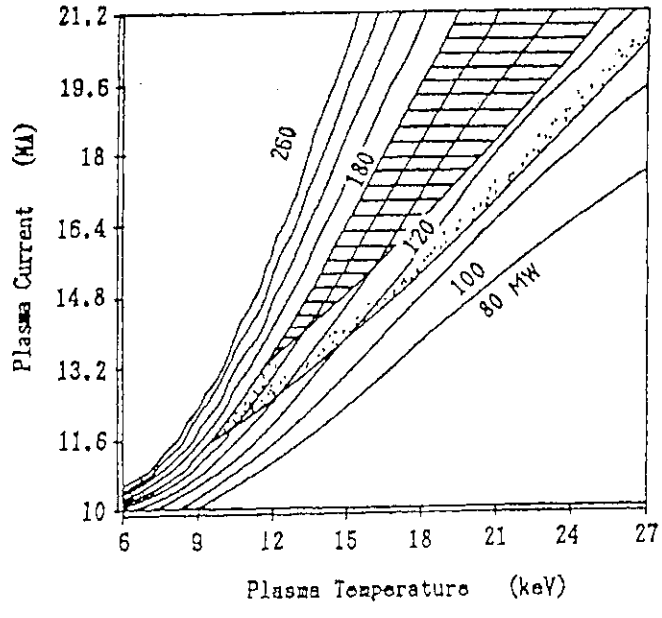

Fig. 27 Contours of equi-required current drive power on the operation space on T-Ip plane for steady state operation with wall loading of 0.8 MW/m^2 for the case of increased toroidal magnetic field of Fig. 26. The required power is reduced substantially due to the extension of operation space toward lower plasma current by the increased toroidal field.

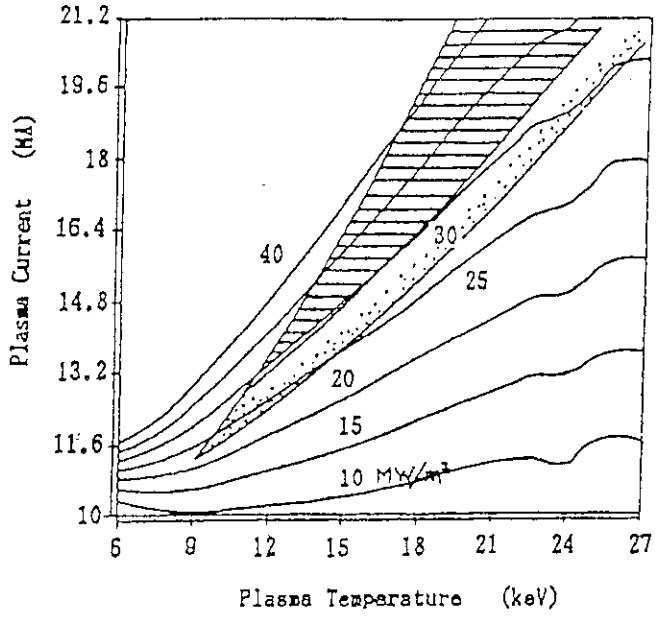

Fig. 28 Contours of equi-divertor heat load on the operation space on T-Ip plane for steady state operation with wall loading of 0.8 MW/m^2 for the case of increased toroidal magnetic field of Fig. 26. The divertor heat load is reduced to some extent due to the extension of operation space toward lower plasma current by the increased toroidal field.